Simulation results of a Canada-wide ocean biogeochemical model including the North Atlantic, North Pacific and Arctic Oceans

James R. Christian, Fiona Davidson, Amber M. Holdsworth, Youyu Lu, Joshua Morgan, Li Zhai, and Zhiyin Zheng

Ocean Sciences Division
Fisheries and Oceans Canada
Institute of Ocean Sciences
9860 West Saanich Road
Sidney, BC
V8L 4B2

2026

Canadian Technical Report of
Fisheries and Aquatic Sciences 3721

Fisheries and Oceans Canada | Pêches et Océans Canada

Canada

Canadian Technical Report of Fisheries and Aquatic Sciences

Technical reports contain scientific and technical information that contributes to existing knowledge but which is not normally appropriate for primary literature. Technical reports are directed primarily toward a worldwide audience and have an international distribution. No restriction is placed on subject matter and the series reflects the broad interests and policies of Fisheries and Oceans Canada, namely, fisheries and aquatic sciences.

Technical reports may be cited as full publications. The correct citation appears above the abstract of each report. Each report is abstracted in the data base *Aquatic Sciences and Fisheries Abstracts*.

Technical reports are produced regionally but are numbered nationally. Requests for individual reports will be filled by the issuing establishment listed on the front cover and title page.

Numbers 1-456 in this series were issued as Technical Reports of the Fisheries Research Board of Canada. Numbers 457-714 were issued as Department of the Environment, Fisheries and Marine Service, Research and Development Directorate Technical Reports. Numbers 715-924 were issued as Department of Fisheries and Environment, Fisheries and Marine Service Technical Reports. The current series name was changed with report number 925.

Rapport technique canadien des sciences halieutiques et aquatiques

Les rapports techniques contiennent des renseignements scientifiques et techniques qui constituent une contribution aux connaissances actuelles, mais qui ne sont pas normalement appropriés pour la publication dans un journal scientifique. Les rapports techniques sont destinés essentiellement à un public international et ils sont distribués à cet échelon. II n'y a aucune restriction quant au sujet; de fait, la série reflète la vaste gamme des intérêts et des politiques de Pêches et Océans Canada, c'est-à-dire les sciences halieutiques et aquatiques.

Les rapports techniques peuvent être cités comme des publications à part entière. Le titre exact figure au-dessus du résumé de chaque rapport. Les rapports techniques sont résumés dans la base de données *Résumés des sciences aquatiques et halieutiques.*

Les rapports techniques sont produits à l'échelon régional, mais numérotés à l'échelon national. Les demandes de rapports seront satisfaites par l'établissement auteur dont le nom figure sur la couverture et la page du titre.

Les numéros 1 à 456 de cette série ont été publiés à titre de Rapports techniques de l'Office des recherches sur les pêcheries du Canada. Les numéros 457 à 714 sont parus à titre de Rapports techniques de la Direction générale de la recherche et du développement, Service des pêches et de la mer, ministère de l'Environnement. Les numéros 715 à 924 ont été publiés à titre de Rapports techniques du Service des pêches et de la mer, ministère des Pêches et de l'Environnement. Le nom actuel de la série a été établi lors de la parution du numéro 925.

Canadian Technical Report of
Fisheries and Aquatic Sciences 3721

2026

SIMULATION RESULTS OF A CANADA-WIDE OCEAN BIOGEOCHEMICAL MODEL INCLUDING THE NORTH ATLANTIC, NORTH PACIFIC AND ARCTIC OCEANS

by

James R. Christian[1], Fiona Davidson[1], Amber M. Holdsworth[1], Youyu Lu[2], Joshua Morgan[1], Li Zhai[2], and Zhiyin Zheng[1]

[1] Fisheries and Oceans Canada
Institute of Ocean Sciences
9860 West Saanich Road
Sidney, BC
V8L 4B2

[2] Fisheries and Oceans Canada
Bedford Institute of Oceanography
PO Box 1006
Dartmouth, NS
B2Y 4A2

Cat. No. Fs 97-6/3721E-PDF ISBN 978-0-660-79079-4 ISSN 1488-5379
https://doi.org/10.60825/hyqd-2f14

Correct citation for this publication:

Christian, J.R., Davidson, F., Holdsworth, A.M., Lu, Y., Morgan, J., Zhai, L., and Zheng, Z. 2026. Simulation results of a Canada-wide ocean biogeochemical model including the North Atlantic, North Pacific and Arctic Oceans. Can. Tech. Rep. Fish. Aquat. Sci. 3721: v + 42 p. https://doi.org/10.60825/hyqd-2f14

TABLE OF CONTENTS

ABSTRACT

Christian, J.R., Davidson, F., Holdsworth, A.M., Lu, Y., Morgan, J., Zhai, L., and Zheng, Z. 2026. Simulation results of a Canada-wide ocean biogeochemical model including the North Atlantic, North Pacific and Arctic Oceans. Can. Tech. Rep. Fish. Aquat. Sci. 3721: v + 42 p. https://doi.org/10.60825/hyqd-2f14

A numerical ocean model with biogeochemistry has been developed for a domain that spans Canada's three oceans: the Atlantic, Pacific and Arctic. The domain extends to 26°N in the Atlantic and 44°N in the Pacific, and spans the full width of each basin as well as the whole of the Arctic Ocean. The resolution is moderate to high (≈0.25°, 75 levels). A series of simulations was conducted to assess the best choices for biogeochemical model parameters across the diverse regions, using a variety of validation data sets including satellite ocean colour (surface chlorophyll and particulate organic carbon, integrated primary production), surface underway pCO_2, and depth profiles of oxygen and nitrate concentration from ships and Argo floats. An extensive set of parameter sensitivity experiments was conducted which are documented in detail here, with a focus on zooplankton grazing and phytoplankton and zooplankton mortality (linear and quadratic) parameters, and particle sedimentation rates. Sensitivity to many of the parameter adjustments examined is low, but the experiments conducted span the range from weak seasonal biological drawdown of surface inorganic carbon and nutrients, to excessively large drawdown and thermocline oxygen demand. Further, the general nonlinearity of the model response to parameter adjustments is shown by similar parameter sets having very different effects on different data metrics. In addition, the model solution's general insensitivity to some phytoplankton processes (exudation, chlorophyll photooxidation) that are neglected in the 'base case' model simulation is demonstrated. An optimal set of parameters for this domain is proposed, but it is possible that there are unexplored regions of the parameter space that could improve performance, especially if additional observational constraints are applied.

RESUMÉ

Christian, J.R., Davidson, F., Holdsworth, A.M., Lu, Y., Morgan, J., Zhai, L., and Zheng, Z. 2026. Simulation results of a Canada-wide ocean biogeochemical model including the North Atlantic, North Pacific and Arctic Oceans. Can. Tech. Rep. Fish. Aquat. Sci. 3721: v + 42 p. https://doi.org/10.60825/hyqd-2f14

Un modèle numérique océanique intégrant la biogéochimie a été développé pour un domaine couvrant les trois océans du Canada : l'Atlantique, le Pacifique et l'Arctique. Ce domaine s'étend jusqu'à 26°N dans l'Atlantique et 44°N dans le Pacifique, et englobe toute la largeur de chaque bassin ainsi que l'océan Arctique dans son intégralité. La résolution est moyenne à élevée (≈0,25°, 75 niveaux). Une série de simulations a été menée afin d'évaluer les paramètres biogéochimiques optimaux pour ces différentes régions, à l'aide de divers ensembles de données de validation, notamment la couleur de l'océan par satellite (chlorophylle de surface et carbone organique particulaire, production primaire intégrée), la pCO_2 de surface en navigation et les profils de concentration d'oxygène et de nitrate mesurés par des navires et des flotteurs Argo. Un ensemble complet d'expériences de sensibilité paramétrique a été réalisé et est documenté en détail ici. Ces expériences portent principalement sur le prédation du zooplancton, la mortalité du phytoplancton et du zooplancton (variations linéaire et quadratique) et les taux de sédimentation des particules. La sensibilité à de nombreux ajustements de paramètres étudiés est faible, mais les expériences menées couvrent un large éventail de situations, allant d'une faible consommation biologique saisonnière du carbone inorganique et des nutriments en surface à une consommation excessive et à une forte demande en oxygène au niveau de la thermocline. De plus, la non-linéarité générale de la réponse du modèle aux ajustements de paramètres est mise en évidence par le fait que des ensembles de paramètres similaires produisent des effets très différents sur différentes métriques. En outre, l'insensibilité générale de la solution du modèle à certains processus phytoplanctoniques (exsudation, photo-oxydation de la chlorophylle) négligés dans la simulation du modèle de référence est démontrée. Un ensemble optimal de paramètres pour ce domaine est proposé, mais il est possible que des régions inexplorées de l'espace des paramètres permettent d'améliorer les performances, notamment en appliquant des contraintes d'observation supplémentaires.

1. INTRODUCTION

An ocean biogeochemical model encompassing Canada's three oceans - the Atlantic, Pacific and Arctic - was developed and used to conduct a series of short (one year) simulations to assess the effect of different parameter choices across regions, and the effect of including additional processes such as fluvial nutrient sources, attenuation by fluvial coloured dissolved organic matter (CDOM), interactive sediments, and iron limitation. The key conclusions of this work were published in a primary literature publication (Christian et al., 2025). In this report we present additional details that can not be accommodated in such a publication.

The vision for such a Canada-wide system was presented in a workshop in February 2021 and the report of that workshop is available at https://drive.google.com/file/d/17VRm9J19K5KvqXjM9IPhkt5UiVYoPKeh/view (Swart et al., 2021). Subsequently, several projects were funded under the DFO Competitive Science Research Fund, which led to several primary publications (Christian et al., 2025; MacDermid et al., 2025). The current contribution describes in detail results of one of those projects.

To break down the task of developing a Canada-wide downscaling system into tractable chunks, work was first begun on evaluating hindcasts with observation-based (reanalysis) atmospheric forcing (e.g., Kobayashi et al., 2015). The model domain is based on the Regional Ice-Ocean Prediction System (RIOPS) (Smith et al., 2021) and extends to 26°N in the Atlantic and 44°N in the Pacific (Figure 1), with a horizontal resolution of ~0.25° (528 x 735) and 75 vertical levels. The grid spans the full width of each basin as well as the whole of the Arctic Ocean. RIOPS is

part of a near-term (<10 days) prediction system that nests three scales: a global prediction system at 1/4°, the 3-Oceans domain at 1/12°, and several high-resolution regional domains (1/36°) on the east and west coasts of Canada (Smith et al., 2021).

The research funded in 2021 and 2022 by DFO took the RIOPS domain as a starting point, expanding its applications to include longer hindcast simulations with reanalysis forcing (MacDermid et al., 2025) and incorporating a biogeochemical model (Christian et al., 2025). For the biogeochemical simulations a resolution of 1/4° was implemented as 1/12° was deemed to be too computationally expensive. An experimental design was defined that consists of a single, arbitrary year of simulation (2017) evaluated against a climatological, or composite, annual cycle in observations. The rationale for such a design is twofold: (1) consultations with the community suggested that the ability to simulate diverse regions with a single set of biology model parameters would be a fundamental weakness for such a Canada-wide modelling system, and (2) in such a highly seasonal mid-to-high latitude environment, the first-order task is to simulate the annual cycle across diverse regions and interannual variability can be neglected. It is also important to note that in all of the parameter experiments the physical ocean is identical, so that model-data agreement for pCO_2, for example, is driven almost entirely by differences in biological uptake of DIC (there are also biological sources and sinks of alkalinity but the primary driver is DIC). The rationale for neglecting interannual variability is further discussed in Christian et al. (2025), along with a partial demonstration that it is indeed second-order.

Validation data were drawn from global, public domain data sets including ocean colour (surface chlorophyll, surface particulate organic carbon (POC), and primary production (PP)), SOCAT

underway pCO_2 and discrete (bottle) samples of O_2 and NO_3^- from Argo and the World Ocean Database (see below Section 2.3). A decision was made not to use gridded data products as these have a native resolution that is coarser than the model grid. Similarly, localized ship-based observations were eschewed in favour of data from data bases that contain observations over a broad swath of regions, although data coverage is poor in some of our validation regions. Nonetheless, these data products provide a fairly robust test of the biogeochemical model parameters, in the sense that some solutions showed a clear signature of too weak or too strong seasonal drawdown of nitrate and DIC, and parameter combinations that were shown to have poor agreement with one data constraint generally had poor agreement with others as well.

2. METHODS

2.1 Model description

The model spans the three contiguous oceans of the northern mid- to high latitudes, including all of the Arctic Ocean, and all of the Pacific and Atlantic north of 44°N and 26°N respectively (Figure 1). The grid is based on the CONCEPTS RIOPS grid (Smith et al., 2021), with a horizontal resolution of ~0.25° (528 x 735) and 75 vertical levels.

The modelling system used is NEMO3.6 (Madec, 2008; Holdsworth et al., 2021; MacDermid et al., 2025); the sea-ice model is LIM3. The biogeochemical model is the Canadian Ocean Ecosystem Model (CanOE) (Christian et al., 2022). All of these components are part of the nemo36mc version archived by Fisheries and Oceans Canada staff at https://gitlab.com/dfo_modcom/nemo36mc. The ocean model is forced at the open boundaries

with the GLORYS4 reanalysis (T, S, u, v); biogeochemical boundary conditions are climatological. Biogeochemical lateral boundary conditions are based on World Ocean Atlas

Figure 1 - Model domain and bathymetry

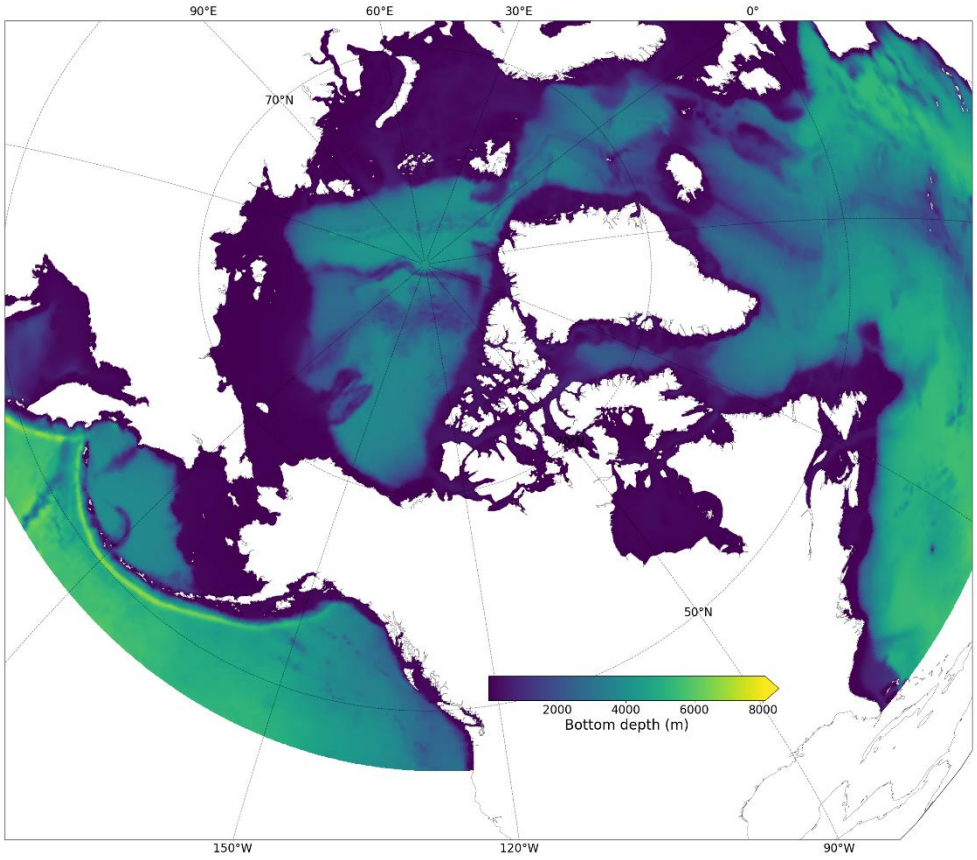

(WOA) 2018 (monthly) for O_2 and NO_3 (Garcia 2018a, b) and the Global Ocean Data Analysis Project (GLODAP) v.2 (annual) for dissolved inorganic carbon (DIC) and alkalinity (Key et al., 2015; Lauvset et al., 2016). Tides are calculated from the Oregon State University TPXO8 global tidal solution (Egbert and Erofeeva, 2002; http://volkov.oce.orst.edu/tides) and include M2, S2, N2, K1 and O1 (cf. MacDermid et al., 2025). Atmospheric forcing is from the Japanese 55-year Reanalysis (JRA55) (Kobayashi et al., 2015) with 3 h resolution. The model time step is 600 s. Biological heat-trapping effects on the physical ocean are neglected. Additional details regarding

the physical ocean and ice model setup are given in MacDermid et al. (2025) and Christian et al. (2025).

The basic set of biogeochemical model parameters is taken from the Coupled Model Intercomparison Project v.6 (CMIP6) simulations with CanESM5-CanOE (Christian et al., 2022; 2025). The suite of mortality coefficients was expanded so that linear and quadratic mortality for large and small phytoplankton and micro- and mesozooplankton can each vary independently. All of these rates exist in CanESM5-CanOE, but in some cases only a single value applied to multiple groups is specified in the original published version (Christian et al., 2022). In the present research, the source code and namelists were modified to allow these to be adjusted independently, for a total of 8 parameter values vs 5 in CanESM5-CanOE (see Table 1), in order to increase the range of possible ecosystem states.

2.2 Validation regions

The model domain was divided into nine regions for model validation: the Eastern Subarctic Pacific (ESP), the Western Subarctic Pacific (WSP), the Bering Sea (BER), the Beaufort Sea (BEAU), the Chukchi Sea (CHUK), northern Baffin Bay (BAFF), the Labrador Sea / Davis Strait (LABR), the Atlantic/Arctic Transition (AATR), and the North Atlantic (NATL) (see Appendix B). These were chosen based on existing literature and consultation with the Canadian oceanography community. The number of regions was kept at what was considered a tractable number (Matrai et al. (2013) have 14 in the Arctic alone) and defined as much as possible based on an expectation of similar oceanographic properties and processes (cf. Henson et al., 2018).

Most of the marginal seas were excluded (e.g., Hudson's Bay and the Sea of Okhotsk), as well as much of the Canadian Arctic Archipelago and the Eurasian coastal region. Exclusion of these regions is due in part to the model resolution, which does not adequately resolve the circulation in these regions, and partly due to unavailability of validation data. The focus is on oceanic regions, along with the broad and relatively open Bering and Chukchi shelves.

2.3 Validation data

Data sets were collected from ocean colour (surface chlorophyll, particulate organic carbon (POC), primary production), Surface Ocean CO_2 Atlas (SOCAT) underway pCO_2 (Bakker et al., 2016; socat.info), biogeochemical Argo floats (O_2 and NO_3) and ship-based profiles of O_2 and NO_3 from the World Ocean Database (WOD) (Boyer et al., 2018). All observations were binned as climatological monthly averages and mapped to the model grid. No gridded data products (e.g., WOA or GLODAP gridded data) were used. For chlorophyll and POC the climatologies from Tesdal et al. (2016) and Stramski et al. (2008) were used as described in Christian et al. (2022; 2025). For primary production, the Carbon, Absorption, and Fluorescence Euphotic-resolving (CAFÉ) data product of Silsbe et al. (2016) was used; five years (2002-2006) were averaged.

2.4 Experimental setup

The standard experiment uses a single, arbitrary year (2017) of atmospheric forcing, with the 'base case' biogeochemical model parameters drawn from CMIP6 experiments on the global

domain with CanESM5-CanOE (Christian et al., 2022). The simulation runs from December 27, 2016 through January 5, 2018, but only data from 2017 are considered in the analysis. Output data are averaged into monthly intervals. The physical model was spun up from an initial state based on GLORYS with a full year of 2016 forcing, followed by another year of 2016 forcing with biogeochemistry, before launching the run with 2017 forcing. Biogeochemical tracers were initialized from WOA (January) and GLODAP (annual); particulates and minor species like NH_4^+ were initialized with a constant value of 0.005 mmol C m^{-3} or its Redfield equivalent. Iron limitation, nitrogen fixation and denitrification were deactivated as these processes are of negligible importance over most of the model domain, although clearly the subarctic Pacific is an exception with repect to iron limitation. Carbon chemistry and air-sea exchange follow the OMIP protocols (Orr et al., 2017). Atmospheric CO_2 concentration is based on the annual mean of observations at Mauna Loa for the period simulated, with an average mid-latitude seasonal cycle superimposed, which is based on data collected at Cape St. James, British Columbia in 1979-1992 (Christian et al., 2025). River water inputs contain DIC and alkalinity at a fixed concentration of 1000 mmol m^{-3} (cf. Tank et al., 2012), but no nitrate or ammonium.

3. RESULTS AND DISCUSSION

A difficulty in this type of publication is the sheer volume of information. Figure 2, for example, shows the model-data agreement for PP over the nine validation regions for the 12 months of the year, for the 'base case' parameter set. If we were to create an Appendix of such plots for each experiment and each validation data set, it could easily run to hundreds of pages. These electronic 'flip books' are useful as a model development and analysis tool. However, for the

current contribution, we attempt to present the key information in as concise a manner as possible.

Figure 2 - Example scatterplots of modelled vs observed primary production for all 12 months of the year. Panels are the nine validation regions; r is the Pearson correlation coefficient.

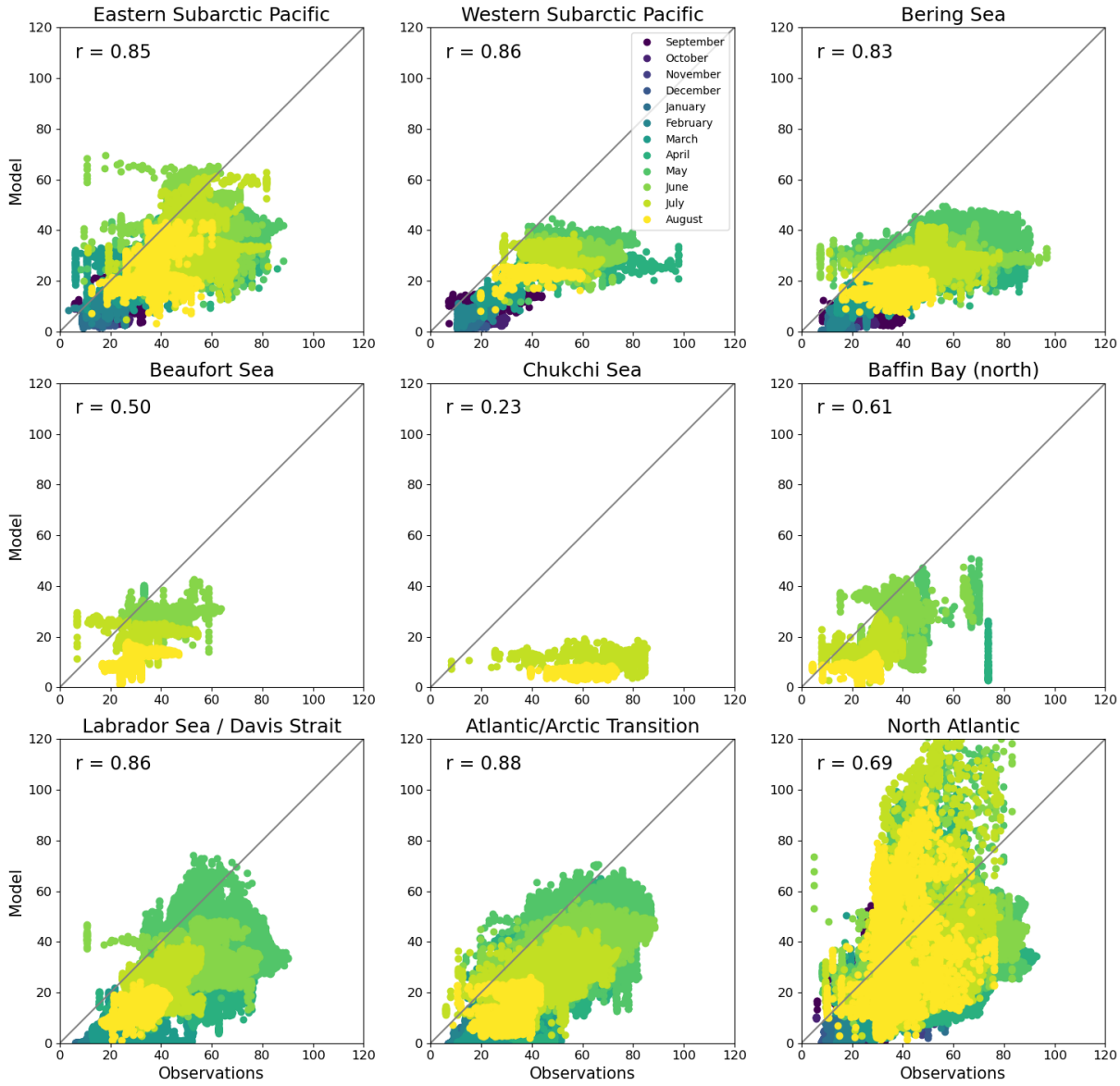

Figure 3 replaces the colour-coded individual months and region-by-region panels in Figure 2 with seasonal (JJAS) means, where the colours represent the regions, so that each experiment occupies only a single panel and up to 20 experiments can be shown on a single page. Figure 3 illustrates the differences among the parameter experiments with regard to variations in primary production within regions. In many cases there are resilient patterns of model bias that are common to a range of experiments, i.e., sensitivity to many of the parameter choices tested is low. However, clearly there are combinations of parameters that push the solution outside of this 'zone of attraction' and into the realm of the opposite bias (e.g., PP is too high where in the majority of experiments it is too low). We had some success in identifying an intermediate case that performs better in most cases across various regions and the full range of observational constraints than the 'bookend' scenarios (Christian et al., 2025). However, as noted by Christian et al. (2025), it remains possible that there are unexplored corners of the parameter space, or other possible model structures, in which sensitivity to other parameters increases.

Heat maps are a useful way of visualizing which experiments stand out as different from the bulk of the others, and also lend themselves to showing many experiments on a single page. Figure 4 shows heat maps for depth-integrated primary production, depth-integrated zooplankton biomass, and phytoplankton community structure ($P_s/(P_s+P_l)$), for a range of experiments varying mortality and grazing parameters (Table 1). The range of outcomes is large, and in some cases outside the bounds of plausibility. Very low zooplankton biomass, on the order of 10 mmolC m^{-2}, is unlikely, so solutions that are dark purple to black on the heat map are excluded. Some of these also perform poorly relative to other data constraints (e.g., Figure 2), but note that the relationship among the different fields is not monotonic: some solutions that have very high

Figure 3 - Scatterplots of summer (JJAS) average modelled vs observed primary production for 37 experiments with varying grazing and mortality parameters (see Table 1). Colors are different regions (continues on next page).

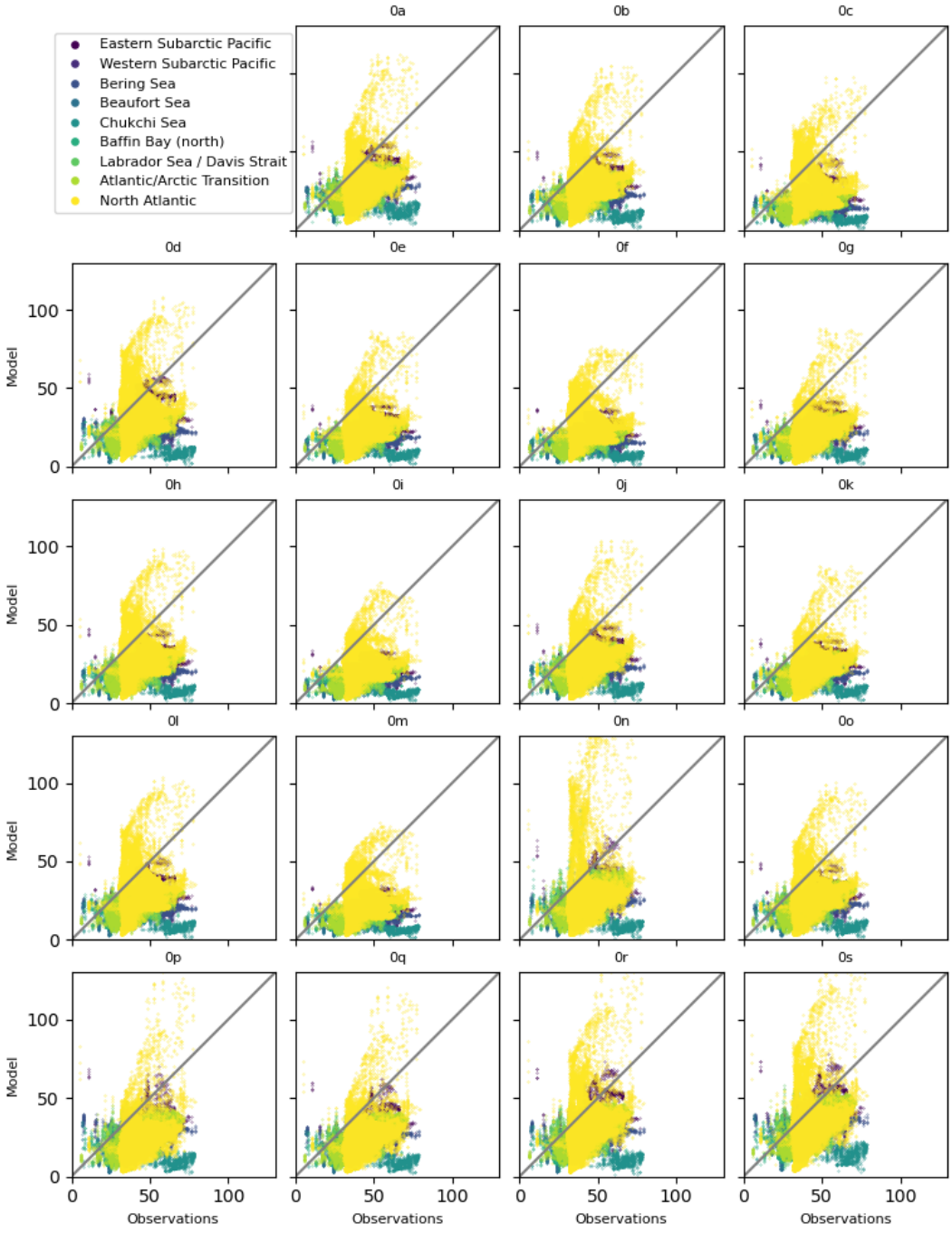

Figure 3 (continued from previous page)

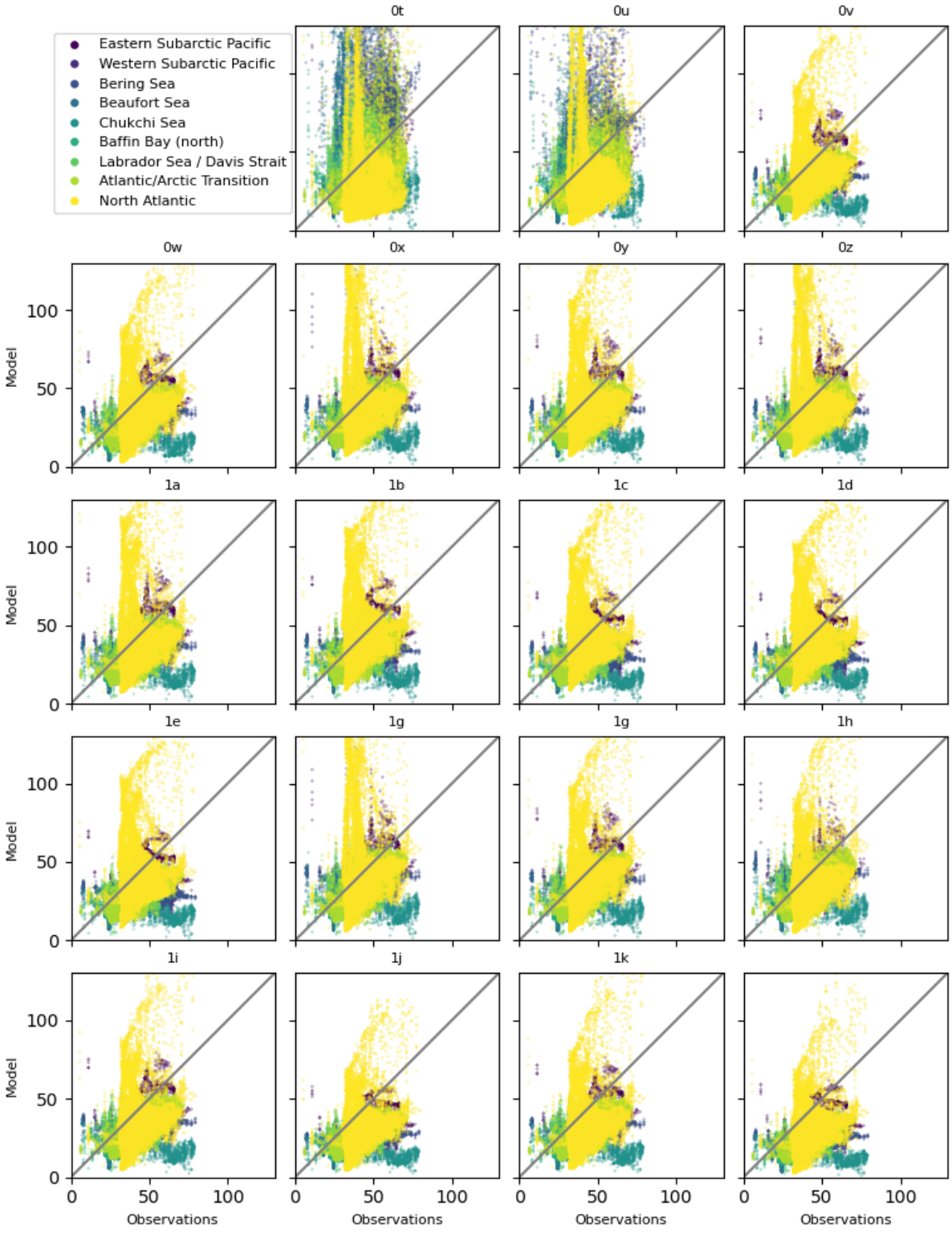

primary production have quite high zooplankton biomass while others have very low zooplankton biomass. The small phytoplankton fraction should be in the vicinity of 0.5, so solutions dominated by one or the other size class (Figure 4) are rejected.

Figure 5 shows similar heat maps for experiments with particle sinking rates (Table 2). This experiment indicates that sensitivity to these parameters is generally low: the results cluster into families of experiments grouped by mortality rate parameters, and there is little variance within these according to the sinking rate. Note that none of these experiments varied the particle remineralization rate; sinking rate and remineralization rate are highly correlated parameters in the sense that increasing or decreasing both by e.g., 30% should produce broadly similar solutions because the sinking and remineralization rate changes cancel each other and the average remineralization length scale (RLS) does not change. All of the experiments shown in Figure 5 involve alteration of the RLS proportional to the sinking rate, yet none shows much sensitivity to this parameter.

Figure 6 shows the mean oxygen concentration at 100-300 m depth for the parameter experiments shown in Figures 3 and 4. Sensitivity is generally low, but a few experiments stand out as having very strong thermocline remineralization, especially in the temperate regions. These are largely experiments that have been found to perform poorly by other criteria (e.g., Figures 3 and 4). Figure 7 shows mean oxygen concentration at 100-300 m depth for the sinking rate experiments shown in Figure 5, grouped (colours) by their 'base case' parameters (Table 2). Again we see that sensitivity to sinking rate is low.

Table 1 - List of grazing/mortality parameter experiments. Experiment codes in column 1 correspond to those used in Figures 3, 4, 6 and 8. First row is CanESM5-CanOE values; subsequent rows contain data only if different from these. Bold indicates experiments 0-7 in Christian et al. (2025). kexh indicates that experiment included exudation and chlorophyll degradation (see below Appendix A).

Expt	gmax1	gmax2	m1ps	m1pl	m1zs	m1zl	m2ps	m2pl	m2zs	m2zl	aps	apl	kexh	Runid*
0a	**1.7**	**0.85**	**0.05**	**0.1**	**0.05**	**0.1**	**0.06**	**0.06**	**0.06**	**0.06**	**0.25**	**0.25**		VJC016q
0b			0.005	0.01	0.005	0.01							Y	VJC014l
0c			0.005	0.01	0.005	0.01					0.5	0.5	Y	VJC014p
0d		1.35	0.005	0.01	0.005	0.01							Y	VJC014q
0e	2.5		0.005	0.01	0.005	0.01							Y	VJC014y
0f	2.5	1.35	0.005	0.01	0.005	0.01							Y	VJC014z
0g	2.5												Y	VJC015e
0h		1.35											Y	VJC015f
0i	2.5	1.35											Y	VJC015g
0j			0.025	0.05	0.025	0.05							Y	VJC015i
0k	2.5		0.025	0.05	0.025	0.05							Y	VJC015j
0l		1.35	0.025	0.05	0.025	0.05							Y	VJC015k
0m	2.5	1.35	0.025	0.05	0.025	0.05							Y	VJC015l
0n							0.006	0.006	0.006				Y	VJC015m
0o										0.006			Y	VJC015n
0p										0.6			Y	VJC015p
0q										0.18			Y	VJC015r
0r	1.2	0.75	0.005	0.01	0.005	0.01							Y	VJC015s
0s	**1.2**	**0.75**	**0.12**	**0.12**	**0.12**	**0.08**								VJC015t
0t	**1.2**	**0.75**	**0.005**	**0.01**	**0.005**	**0.01**	**0.002**	**0.002**	**0.002**	**0.3**				VJC015u
0u			**0.12**	**0.12**	**0.12**	**0.08**	**0.002**	**0.002**	**0.002**	**0.3**				VJC015v
0v	**1.2**	**0.75**	**0.005**	**0.01**	**0.005**	**0.01**								VJC015w
0w	1.2	0.75	0.12	0.12	0.12	0.08				0.006				VJC016c
0x	1.2	0.75	0.005	0.01	0.005	0.01		0.006						VJC016d
0y	1.2	0.75	0.005	0.01	0.005	0.01		0.02						VJC016g
0z	1.2	0.75	0.005	0.01	0.005	0.01		0.03						VJC016h

1a	1.2	0.75	0.005	0.01	0.005	0.01		0.012						VJC016i
1b	1.2	0.75	0.005	0.01	0.005	0.01		0.012		0.012				VJC016j
1c	1.5	0.75	0.005	0.01	0.005	0.01		0.012		0.012				VJC016k
1d	1.5	0.75	0.015	0.01	0.005	0.01		0.012		0.012				VJC016l
1e	1.5	0.75	0.025	0.01	0.005	0.01		0.012		0.012				VJC016m
1f	**1.2**	**0.75**		**0.01**		**0.01**		**0.006**						VJC016n
1g	**1.2**	**0.75**		**0.01**		**0.01**		**0.03**						VJC016o
1h	**1.2**	**0.75**		**0.01**		**0.01**		**0.03**		**0.12**				VJC016p
1i	1.2	0.75		0.05		0.05								VJC016r
1j				0.05		0.05								VJC016s
1k	1.2	0.75												VJC016t

* Runid's are the actual run code names included for reference of readers who wish to check original data or namelists on GPSC (namelists can be found in /home/stod000/control/CREG025_LIM3_CANOE-${Runid}/, raw output data in /gpfs/fs7/dfo/hpcmc/comda/stod000/RUN_DIR/Auto-restart/CREG025_LIM3_CANOE/CREG025_LIM3_CANOE-${Runid}/CDF

Figure 4 - Heat maps for integrated primary production, integrated mesozooplankton biomass, and phytoplankton community structure ($P_s/(P_s+P_l)$) for 37 experiments with varying grazing and mortality parameters (see Table 1).

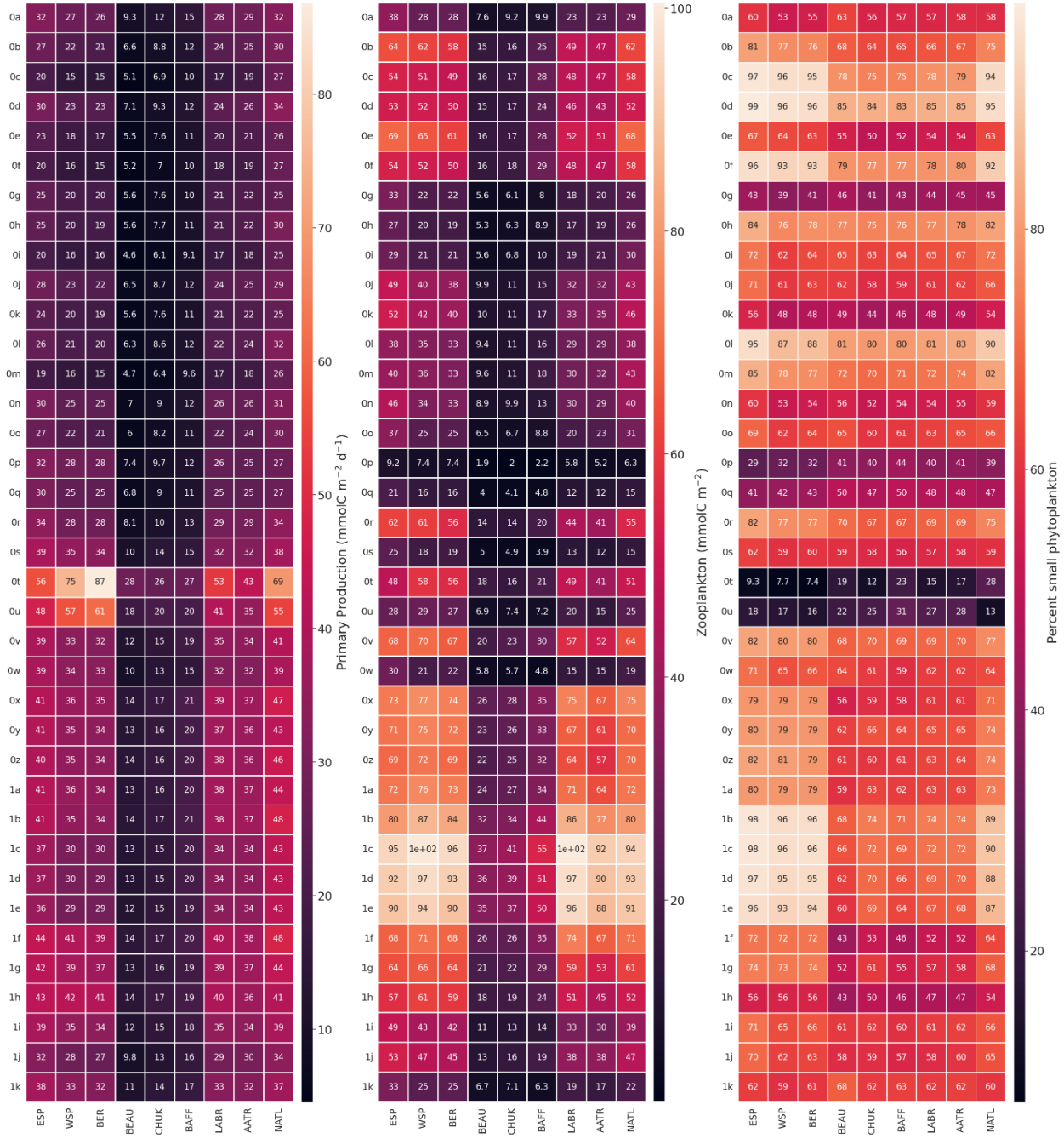

Figure 5 - Heat maps for integrated primary production, integrated mesozooplankton biomass, and phytoplankton community structure ($P_s/(P_s+P_l)$) for experiments with varying particle sinking rates (see Table 2).

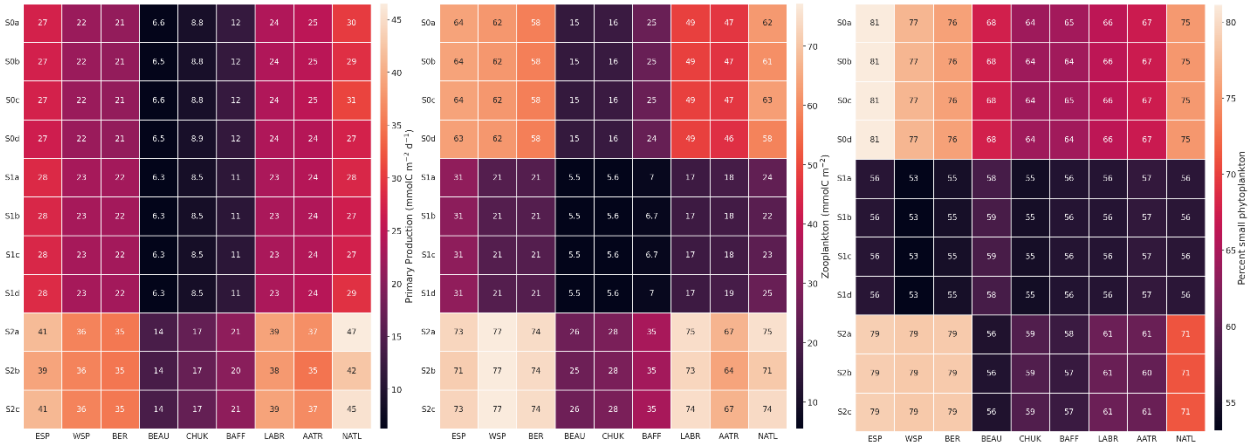

Table 2 - List of sinking rate parameter experiments. Experiment codes in column 1 correspond to those used in Figures 5 and 7. 'Point of departure' runs (S0x) vary somewhat in their parameter choices; other runs in that family (SNx, N=1,3) are identical except for sinking rates. Sinking rates are in m d^{-1}. All S0 experiments have the CanESM5-CanOE values of w_s=2 m d^{-1} and w_l = 30 m d^{-1}. S0a corresponds to 0b in Table 1 and S0c to 0x. S0b is not listed in Table 1 because it corresponds to 0a plus exudation and chlorophyll degradation; all S0 and S1 experiments have these processes active. Runid's are explained in Table 1.

	w_s	w_l	Runid
S0a			VJC014l
S1a	3	20	VJC014m
S2a	2	20	VJC014n
S3a	10	10	VJC014o
S0b			VJC015a
S1b	3	40	VJC015b
S2b	3	30	VJC015c
S3b	2	20	VJC015d
S0c			VJC016d
S1c	4	20	VJC016e
S2c	2	50	VJC016f

Figure 6 - Region mean dissolved oxygen concentration averaged from 100-300 m for 37 experiments with varying grazing and mortality parameters (see Table 1).

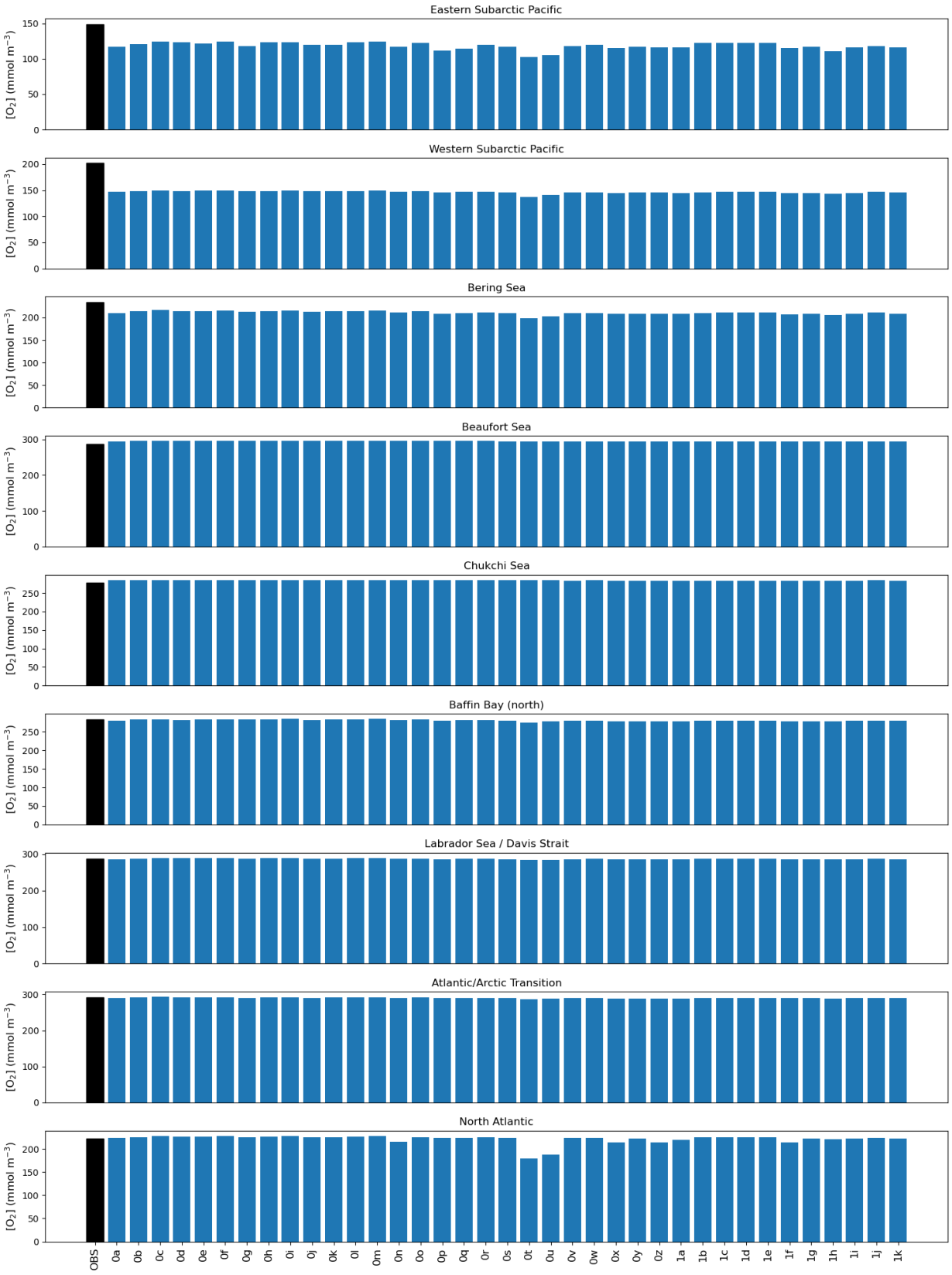

Figure 7 - Region mean dissolved oxygen concentration averaged from 100-300 m for experiments with varying particle sinking rates; experiments are colour-coded by base case model parameters (see Table 2).

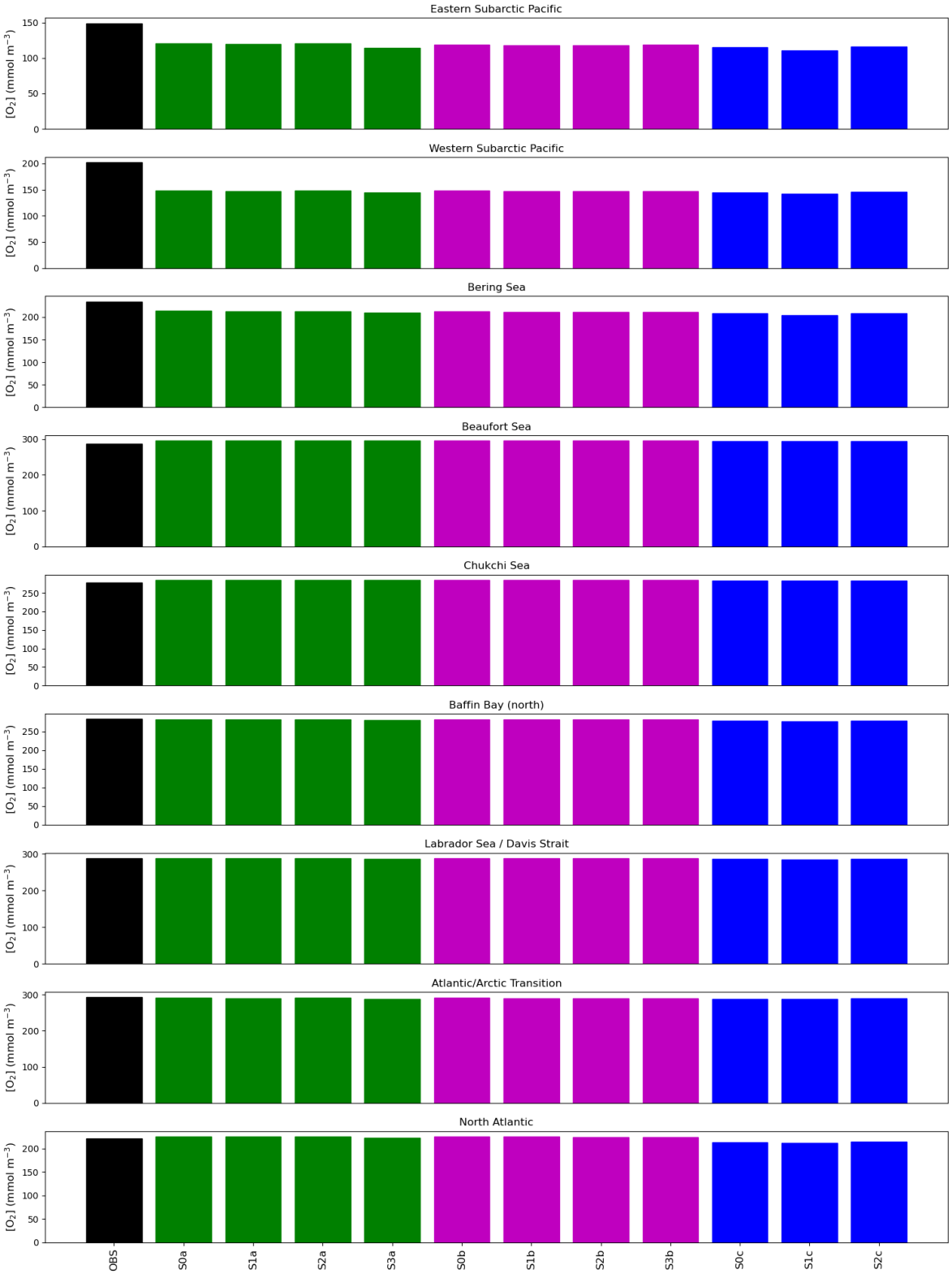

Figure 8 shows the relationship between measures of the accuracy of the modelled spatial distribution (spatial pattern correlation coefficient, r) and accuracy with respect to the mean value (root mean square error, RMS) for four observational data sets: surface nitrate (NO3) concentration, surface chlorophyll concentration (CHL), depth-integrated primary production

Figure 8 - Relationship between model bias (root-mean-square (RMS) error) and spatial pattern correlation across regions for surface nitrate concentration, surface chlorophyll concentration, integrated primary production, and surface pCO_2. Square symbols represent the 'base case' parameter sets for the sinking-rate sensitivity experiments (Table 2).

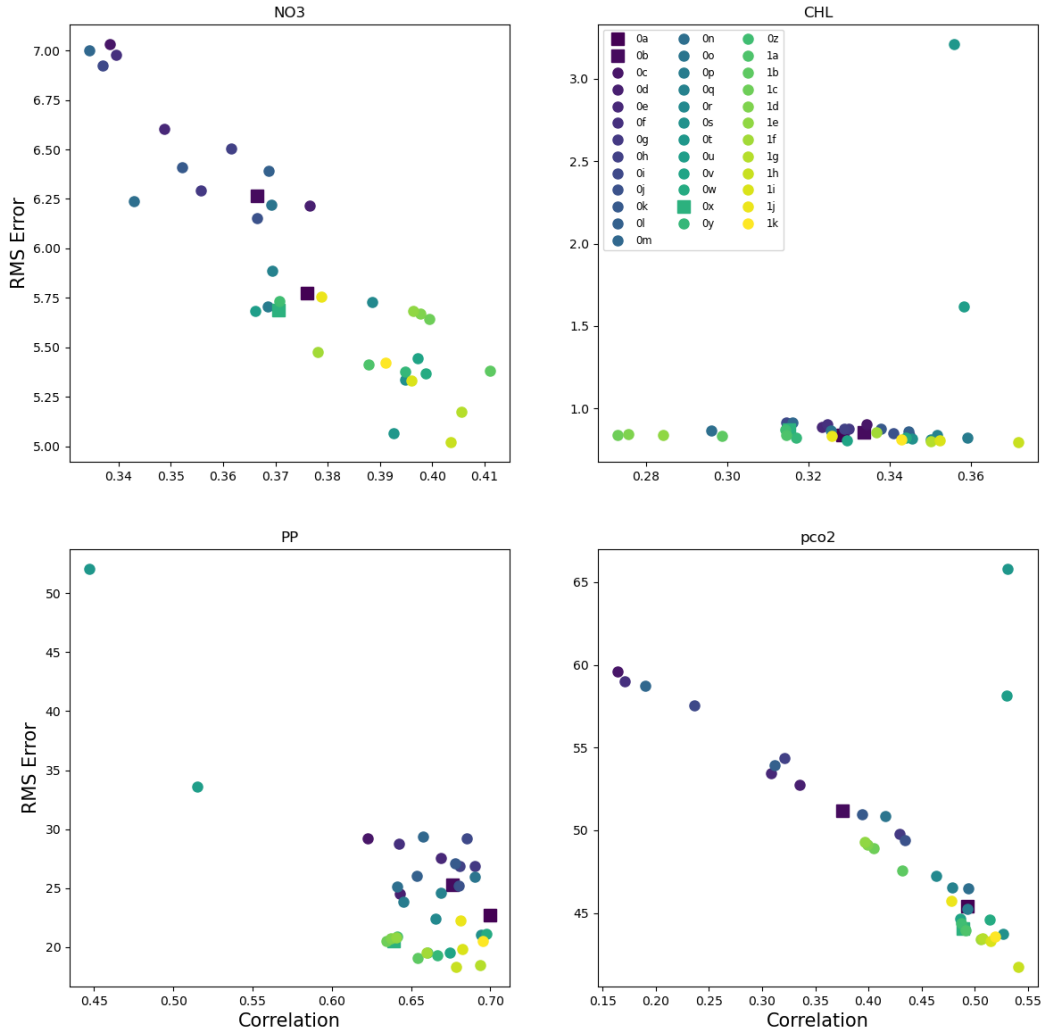

(PP), and surface partial pressure of CO_2 (pCO_2). We see a range of outcomes: for NO_3 and pCO_2, r and RMS are strongly negatively correlated (solutions that best reproduce the mean concentration also have stronger spatial correlation). PP and chlorophyll show much weaker correlation between r and RMS; most of the solutions are similar except for a few outliers. However, it is also important to consider the range of values: NO_3 and pCO_2 show a similar correlation between r and RMS, but for NO_3 the range of r is small; for pCO_2 it is much larger. The handful experiments that stand out on most of these plots generally have poor skill relative to these metrics, but for pCO_2 they have high pattern correlation (as well as high RMS). In the case of chlorophyll, the sensitivity of the RMS is generally low; both r and RMS show quite narrow ranges except for a few outliers, and are weakly correlated. Generally, the solutions that appear as outliers on these plots are the same ones that also perform poorly relative to other metrics (see above Figures 3-6).

4 - CONCLUSION

Results are presented here that are complementary to a primary literature publication (Christian et al., 2025), to expand on details that can not be accommodated in such a publication. In that publication we focused on a limited set of 'bookend' scenarios: (1) the 'base case', based on the global model CanESM5-CanOE (Christian et al., 2022), which has weak seasonal drawdown of NO_3 and DIC, (2) a 'diatom-dominated' community based on a continental shelf environment, which has excessively strong seasonal drawdown and thermocline O_2 demand, and (3) several 'Goldilocks' solutions that fall in between these extremes and represent the best compromise parameter set over the broad and diverse regions within our model domain. That publication also

contains results of a set of experiments where additional processes were considered that are otherwise neglected: fluvial nutrient sources, attenuation by fluvial CDOM, interactive sediments, and iron limitation. In this publication we show the results of a much broader suite of parameter experiments, many of which are very similar to the 'base case', as it took some trial and error to determine which parameter choices would move the solution in the direction of stronger seasonal drawdown. The (high-dimensional) parameter space has not been thoroughly explored, and it is possible that in some unexamined corner of it other solutions exist that are equal to, or more skillful than, the ones we have so far identified as optimal. It is also possible (or even probable) that our conclusions regarding sensitivity (or not) to additional processes are somewhat contingent on the parameter set used, and could be revised if those experiments were repeated with other parameter sets. An exhaustive suite of such experiments is not possible; we document here the ones we have done so that they are in the public record.

Using a composite seasonal cycle is a practical necessity that is unlikely to alter the key results very much. The annual cycle accounts for a large part of the variance in upper ocean properties over much of the world ocean, especially in the mid-to-high latitudes (e.g., Yashayaev and Zveryaev, 2001). A limited test with several successive years (2015-2017) of atmospheric forcing showed that the differences are indeed small compared to the differences among parameters sets, at least for the skill metrics we employed (Christian et al., 2025). In our domain, however, secular (anthropogenic) trends must also be considered. These may be a larger source of error, especially in high latitude regions. Sea ice cover has a strong long-term downward trend (Meredith et al., 2019). In some cases, there is large gap between the years for which observational data are available and the year simulated (more than ten years in the case of PP). It

is likely that PP has increased, or the highest rates ocur occur earlier in the year, in some regions. An example of the consequences of such changes in seasonality is discussed in Christian et al. (2025), whereby earlier retreat of sea ice may have affected the seasonality of primary productivity in high-latitude regions, causing a mismatch with the observation-based estimates, which are available only for a very limited period in summer. Once again, we appeal to practical necessity and the need to focus first on the processes responsible for the largest part of the variance in assessing first the seasonal and regional differences, while remaining aware of the limitations of this strategy. Hopefully, interannual hindcasts with biogeochemistry will be available for evaluation in the near future, although it will probably be impractical to repeat them with multiple parameter sets.

In general, a key conclusion of this work is that sensitivity to most of the parameter choices tested is low for the observational data sets examined. The primary literature publication focused on the 'bookend' scenarios that showed greatest sensitivity, particularly with respect to major tracers like oxygen and dissolved inorganic carbon (DIC); the broader range of experiments is documented here for the benefit of other investigators who may be contemplating using this or similar models. The reason why many of the solutions are very similar, and not particularly skillful, is that initially we made only incremental adjustments from the base case, and made possibly naive assumptions about which parameters the solution would be sensitive to. Sinking rates in particular proved to be less important than originally anticipated (Figures 5 and 7). Community structure appears to be a key determinant of seasonal biological drawdown, and is quite sensitive to grazing and mortality parameters. To find the "Goldilocks" solutions required both adjusting parameter values farther from the base case than anticipated and altering the

source code to expand the suite of parameters that can vary independently. The "Goldilocks" solutions represent only a small fraction of the parameter sets tested so far, but can be used as a base for further experimentation.

5 - ACKNOWLEDGMENTS

This research was funded in part by Fisheries and Oceans Canada through the Competitive Science Research Fund. We thank the numerous data originators who contributed data to the various data products used, and the data centres who maintain these products. We are grateful to Sarah MacDermid, Cathy Reader, Benjamin Richaud, and Nadja Steiner for sea ice data and useful discussions about sea ice modelling and Arctic oceanography, to all of the participants in our experimental design workshop, and to Akash Sastri for useful discussions about mesozooplankton abundance. Nicolas Lambert contributed extensively to the development and archiving of nemo36mc. Figure 1 was drawn with a script modified from one written by Antoine Haddon.

6 - LITERATURE CITED

Bakker, D., Pfeil, B., Landa, C., Metzl, N., O'Brien, K., Olsen, A., Smith, K., Cosca, C., Harasawa, S., Jones, S., Nakaoka, S., Nojiri, Y., Schuster, U., Steinhoff, T., Sweeney, C., Takahashi, T., Tilbrook, B., Wada, C., Wanninkhof, R., Alin, S., Balestrini, C., Barbero, L., Bates, N., Bianchi, A., Bonou, F., Boutin, J., Bozec, Y., Burger, E., Cai, W., Castle, R., Chen, L., Chierici, M., Currie, K., Evans, W., Featherstone, C., Feely, R., Fransson, A., Goyet, C., Greenwood, N., Gregor, L., Hankin, S., Hardman-Mountford, N., Harlay, J., Hauck, J., Hoppema, M., Humphreys, M., Hunt, C., Huss, B., Ibanhez, J., Johannessen, T., Keeling, R., Kitidis, V., Kortzinger, A., Kozyr, A., Krasakopoulou, E., Kuwata, A., Landschutzer, P., Lauvset, S., Lefevre, N., Lo Monaco, C., Manke, A., Mathis, J., Merlivat, L., Millero, F., Monteiro, P., Munro, D., Murata, A., Newberger, T., Omar, A., Ono, T., Paterson, K., Pearce,

D., Pierrot, D., Robbins, L., Saito, S., Salisbury, J., Schlitzer, R., Schneider, B., Schweitzer, R., Sieger, R., Skjelvan, I., Sullivan, K., Sutherland, S., Sutton, A., Tadokoro, K., Telszewski, M., Tuma, M., van Heuven, S., Vandemark, D., Ward, B., Watson, A., and Xu, S. 2016. A multi-decade record of high-quality fCO_2 data in version 3 of the Surface Ocean CO_2 Atlas (SOCAT). Earth System Science Data **8**(2): 383-413.

Boyer, T.P., Baranova, O.K., Coleman, C., Garcia, H.E., Grodsky, A., Locarnini, R.A. Mishonov, A.V., Paver, C.R. Reagan, J.R., Seidov, D., Smolyar, I.V., Weathers, K., and Zweng, M.M. 2018. World Ocean Database 2018. A.V. Mishonov, Technical Ed., NOAA Atlas NESDIS 87.

Christian, J.R., Denman, K.L., Hayashida, H., Holdsworth, A.M., Lee, W.G., Riche, O.G.J., Shao, A.E., Steiner, N., and Swart, N.C. 2022. Ocean biogeochemistry in the Canadian Earth System Model version 5.0.3: CanESM5 and CanESM5-CanOE. Geoscientific Model Development **15**(11) 10.5194/gmd-15-4393-2022

Christian, J.R., Davidson, F., Holdsworth, A.M., Lu, Y., Morgan, J., Zhai, L., and Zheng, Z 2026. A Canada-wide ocean biogeochemical model encompassing the North Atlantic, North Pacific and Arctic Oceans. Atmosphere-Ocean **64**(1): 77–99.

Egbert, G., and Erofeeva, S. 2002. Efficient inverse Modeling of barotropic ocean tides. Journal of Atmospheric and Oceanic Technology **19**(2): 183-204.

Garcia, H.E., Weathers, K., Paver, C.R., Smolyar, I., Boyer, T.P., Locarnini, R.A., Zweng, M.M., Mishonov, A.V., Baranova, O.K., Seidov, D., and Reagan, J.R. 2018a. World Ocean Atlas 2018, Volume 3: Dissolved Oxygen, Apparent Oxygen Utilization, and Oxygen Saturation. A. Mishonov Technical Ed., NOAA Atlas NESDIS 83, 38 pp.

Garcia, H.E., Weathers, K., Paver, C.R., Smolyar, I., Boyer, T.P., Locarnini, R.A., Zweng, M.M., Mishonov, A.V., Baranova, O.K., Seidov, D., and Reagan, J.R. 2018b. World Ocean Atlas 2018, Volume 4: Dissolved Inorganic Nutrients (phosphate, nitrate and nitrate+nitrite, silicate). A. Mishonov Technical Ed., NOAA Atlas NESDIS 84, 35 pp.

Henson, S., Humphreys, M., Land, P., Shutler, J., Goddijn-Murphy, L., and Warren, M. 2018. Controls on Open-Ocean North Atlantic pCO_2 at Seasonal and Interannual Time Scales Are Different. Geophysical Research Letters **45**(17): 9067-9076.

Holdsworth, A., Zhai, L., Lu, Y., and Christian, J. 2021. Future Changes in Oceanography and Biogeochemistry Along the Canadian Pacific Continental Margin. Frontiers in Marine Science **8**. 10.3389/fmars.2021.602991

Key, R.M., Olsen, A., van Heuven, S., Lauvset, S. K., Velo, A., Lin, X., Schirnick, C., Kozyr, A., Tanhua, T., Hoppema, M., Jutterström, S., Steinfeldt, R., Jeansson, E., Ishii, M., Perez, F. F., and Suzuki, T. 2015. Global Ocean Data Analysis Project, Version 2 (GLODAPv2), ORNL/CDIAC-162, NDP-093. Carbon Dioxide Information Analysis Center, Oak Ridge National Laboratory, US Department of Energy, Oak Ridge, Tennessee.

doi:10.3334/CDIAC/OTG.NDP093_GLODAPv2

Kobayashi, S., Ota, Y., Harada, Y., Ebita, A., Moriya, M., Onoda, H., Onogi, K., Kamahori, H., Kobayashi, C., Endo, H., Miyaoka, K., and Takahashi, K. 2015. The JRA-55 Reanalysis: General Specifications and Basic Characteristics. Journal of the Meteorological Society of Japan **93**(1): 5-48.

Lauvset, S., Key, R., Olsen, A., van Heuven, S., Velo, A., Lin, X., Schirnick, C., Kozyr, A., Tanhua, T., Hoppema, M., Jutterstrom, S., Steinfeldt, R., Jeansson, E., Ishii, M., Perez, F., Suzuki, T., and Watelet, S. 2016. A new global interior ocean mapped climatology: the 1 degrees x 1 degrees GLODAP version 2. Earth System Science Data **8**(2): 325-340.

MacDermid, S., Lu, Y., Hu, X., and Brickman, D. 2025. Tuning ice model parameters to improve Arctic sea-ice simulation using the ERA5 atmospheric reanalysis forcing. Journal of Operational Oceanography 18(1): 59-73.

Madec, G. 2008. NEMO ocean engine. Note du pôle de modélisation. Institut Pierre-Simon Laplace (IPSL).

Matrai, P., Olson, E., Suttles, S., Hill, V., Codispoti, L., Light, B., and Steele, M. 2013. Synthesis of primary production in the Arctic Ocean: I. Surface waters, 1954-2007. Progress in Oceanography **110**: 93-106.

Meredith, M., Sommerkorn, M., Cassotta, S., Derksen, C., Ekaykin, A., Hollowed, A., Kofinas, G., Mackintosh, A., Melbourne-Thomas, J., Muelbert, M.M.C., Ottersen, G., Pritchard, H., and Schuur, E.A.G. 2019. Polar regions. pp. 203–320 in H.-O. Pörtner, D.C. Roberts, V. Masson-Delmotte, P. Zhai, M. Tignor, E. Poloczanska, K. Mintenbeck, A. Alegría, M. Nicolai, A. Okem, J. Petzold, B. Rama & N.M. Weyer (Eds.) IPCC Special Report on the Ocean and Cryosphere in a Changing Climate.

Orr, J.C., Najjar, R.G., Aumont, O., Bopp, L., Bullister, J.L., Danabasoglu, G., Doney, S.C., Dunne, J.P., Dutay, J.C., Graven, H., Griffies, S.M., John, J.G., Joos, F., Levin, I., Lindsay, K., Matear, R.J., McKinley, G.A., Mouchet, A., Oschlies, A., Romanou, A., Schlitzer, R., Tagliabue, A., Tanhua, T., and Yool, A. 2017. Biogeochemical protocols and diagnostics for the CMIP6 Ocean Model Intercomparison Project (OMIP). Geoscientific Model Development **10**(6): 2169-2199.

Silsbe, G., Behrenfeld, M., Halsey, K., Milligan, A., and Westberry, T. 2016. The CAFE model: A net production model for global ocean phytoplankton. Global Biogeochemical Cycles **30**(12): 1756-1777.

Smith, G.C., Liu, Y.M., Benkiran, M., Chikhar, K., Colan, D.S., Gauthier, A.A., Testut, C.E., Dupont, F., Lei, J., Roy, F., Lemieux, J.F., and Davidson, F. 2021. The Regional Ice Ocean Prediction System v2: a pan-Canadian ocean analysis system using an online tidal harmonic analysis. Geoscientific Model Development **14**(3): 1445-1467.

Stramski, D., Reynolds, R., Babin, M., Kaczmarek, S., Lewis, M., Rottgers, R., Sciandra, A., Stramska, M., Twardowski, M., Franz, B., and Claustre, H. 2008. Relationships between the surface concentration of particulate organic carbon and optical properties in the eastern South Pacific and eastern Atlantic Oceans. Biogeosciences **5**(1): 171-201.

Swart, N., Holdsworth, A., Steiner, N., and Christian, J., eds. 2021. CanTODS February 2021 workshop report. available at https://drive.google.com/file/d/17VRm9J19K5KvqXjM9IPhkt5UiVYoPKeh/view

Tank, S., Raymond, P., Striegl, R., McClelland, J., Holmes, R., Fiske, G., and Peterson, B. 2012. A land-to-ocean perspective on the magnitude, source and implication of DIC flux from major Arctic rivers to the Arctic Ocean. Global Biogeochemical Cycles **26**.

Tesdal, J., Christian, J., Monahan, A., and von Salzen, K. 2016. Evaluation of diverse approaches for estimating sea-surface DMS concentration and air-sea exchange at global scale. Environmental Chemistry **13**(2): 390-412.

Yashayaev, I., and Zveryaev, I. 2001. Climate of the seasonal cycle in the North Pacific and the North Atlantic Oceans. International Journal of Climatology 21(4): 401-417.

APPENDIX A - EXUDATION AND CHLOROPHYLL DEGRADATION

The limited suite of experiments presented in Christian et al. (2025), was based on the parameters used in CMIP6 simulations with CanESM5-CanOE (Christian et al., 2022), but with exudation, chlorophyll photooxidation and iron limitation deactivated. Other experiments were conducted before the decision was made to exclude these processes, and in some cases an exact 'apples to apples' comparison is not possible, e.g., experiment A has exudation and experiment B does not, but there are also differences in other parameters. However, the differences attributable strictly to exudation (kexh) and/or photooxidation (degr) are small and there is still informational value in these comparisons. So repeating all of the experiments with each combination of +/- kexh, +/- degr was deemed to be a poor use of resources.

Figure A1 shows a set of heat maps for two sets of experiments with exudation and chlorophyll degradation activated or deactivated. Two sets of experiments are shown, ED0abcd and ED1abcd with (a) signifying neither process is active, (b) having exudation only, (c) having chlorophyll degradation only and (d) having both. ED0 and ED1 correspond to experiments 0a and 0b in Table 1, that is, ED0 has higher linear mortalities and other parameters are the same; the other six experiments are not considered elsewhere in this report. Primary production, zooplankton biomass and small phytoplankton fraction all increase slightly as result of deactivating these processes. The differences are small; patterns across regions are largely unaffected, and the differences are generally much smaller than the differences between ED0 and ED1 that are robust across the four sub-experiments. Figure A2 shows a cross region model-data comparison for pCO_2, surface nitrate and surface chlorophyll for one of these sets of four experiments (ED0); the differences are barely detectable. We conclude that these processes are unnecessary for this

domain, and that the comparisons across parameter experiments shown above (e.g., Figures 3-7) are valid despite including some configurations that include these processes and others that do not (Table 1). The influence of these processes on the results shown is second-order for this domain.

Figure A1 - Heat maps for integrated primary production, integrated mesozooplankton biomass, and phytoplankton community structure ($P_s/(P_s+P_l)$) for experiments with and without exudation and chlorophyll degradation. ED0 and ED1 correspond to experiments 0a and 0b in Table 1. EDXa = neither exudation nor degradation; EDXb = exudation only; EDXc = degradation only; EDXa = both.

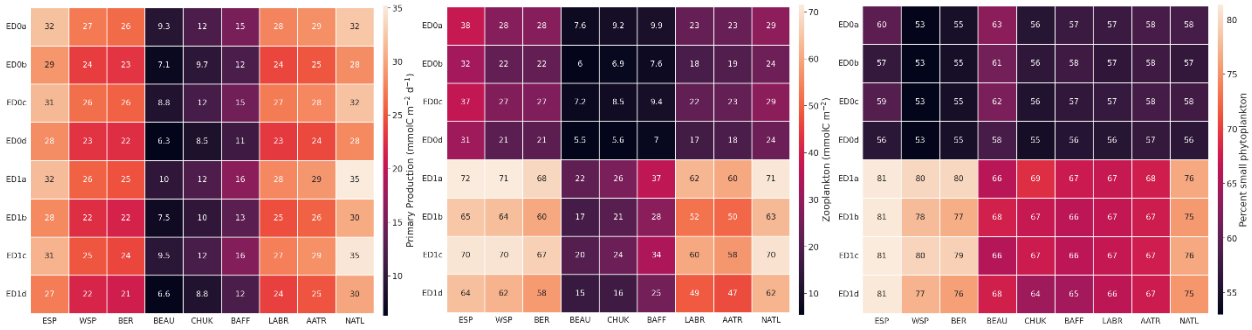

Figure A2 - Scatter plots for regional mean surface pCO_2, nitrate concentration and chlorophyll concentration and for experiments with and without exudation (kexh) and chlorophyll degradation (degr). Base case (experiment with neither process) is experiment 0a in Table 1.

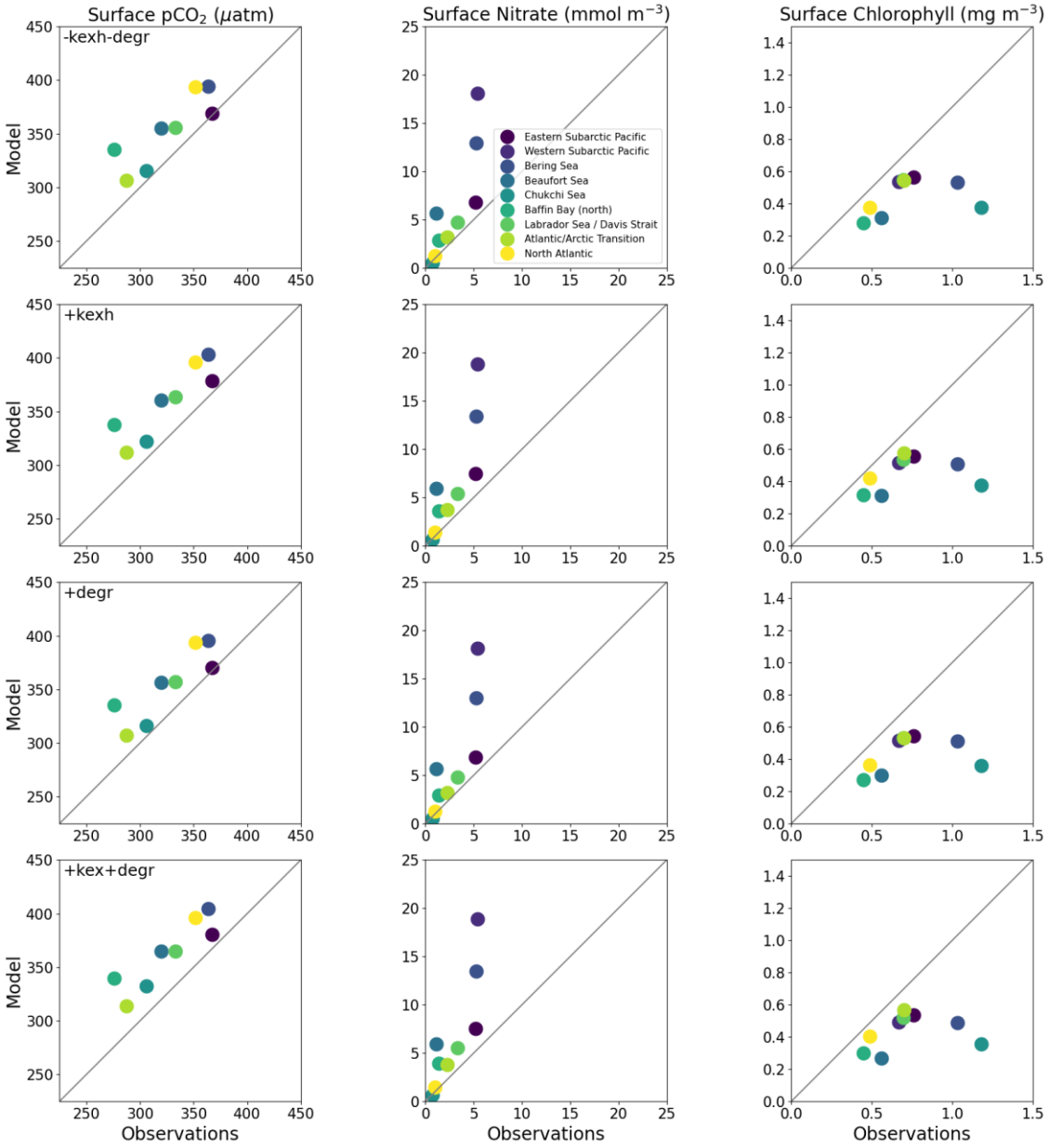

APPENDIX B - DEFINITION OF VALIDATION REGIONS

The regions were defined in consultation with the Canadian oceanographic community, and are somewhat ad hoc, i.e., there is no real theory guiding the exact positions of the boundaries. There is, however, a consistent set of principles that were drawn on: regions like the Sea of Okhotsk, Hudson's Bay, and the Canadian Arctic Archipelago are not well resolved at 0.25° resolution and are therefore excluded. Much of the coastal area on the Eurasian side of the Arctic was excluded for the same reason but also partly due to the general lack of observational data. However, the exact locations of the inter-region boundaries and the exclusion regions are in a sense 'hand drawn' (by directly specifying ranges of grid indices). So the full script is reproduced here for traceability.

Figure B1 - Map of validation regions

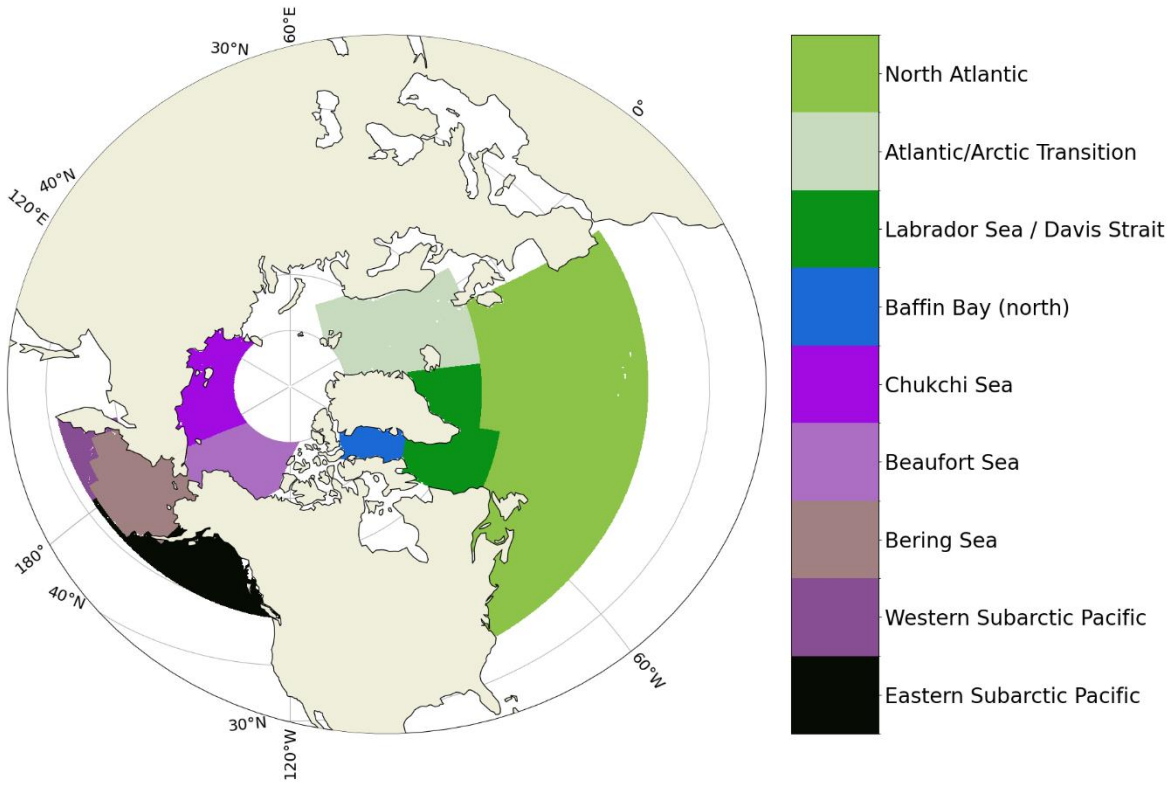

```
filein='coordinates_CREG025_LIM.nc';
X=ncread(filein,'nav_lon'); Y=ncread(filein,'nav_lat'); [nx ny]=size(X);

ewb=250; ewbm1=ewb-1;            % grid index for dividing east and west
ibs=212; jbs=600; jalc=696;      % grid indices for position of Bering Strait
and Aleutian island chain
jstg=171;                        % grid index for dividing North Atlantic
from subarctic: see Henson et al 2018 Fig 1 (189 is the southern tip of
Greenland)
istk=328; jstk=700;              % grid indices for southern tip of Kamchatka
istg=214;
jds=254;

mask=X*0; mask(1:ewbm1,jbs:ny)=1; mask(ewb:nx,jbs:ny)=2;
% Bering Sea (needs fine-tuning)
i=(ibs-10):(ibs+50); j=jbs:jalc; mask(i,j)=3;
i=(ibs-20):(ibs+70); j=jbs:(jalc-10); mask(i,j)=3;
i=(ibs-40):(ibs+90); j=jbs:(jalc-20); mask(i,j)=3;
mask(1:ewbm1,350:599)=4;
mask(ewb:nx,350:599)=5;

mask(1:ewbm1,jstg:349)=7;
mask(210:nx,jstg:349)=8;
mask(:,1:(jstg-1))=9;
mask(1:istg,151:349)=7;
mask(istg:280,jstg:250)=7;
mask(1:istg,jds:349)=6;

% marginal seas mask
mask(347:nx,1:jstg)=nan;    % Med
mask(385:nx,150:263)=nan;  % Baltic
% exclude Russian coastal region west of the Laptev Sea
mask(405:nx,275:460)=nan;
for i=1:60, j=350+i; k=350:(350+4*i); mask(j,k)=nan; end
mask(380:410,490:520)=5;
% SoO
mask(330:nx,jbs:ny)=nan;
for i=istk:(istk+ny-jstk),
 j=(jstk+i-istk):ny; mask(i,j)=2;
end
mask(315:nx,615:680)=nan; mask(290:nx,615:646)=nan;
% HB and CAA
mask(1:135,150:470)=nan; mask(1:150,250:400)=nan; mask(1:120,150:550)=nan;
mask(155:238,350:380)=nan;
for i=125:235, j=375:(615-i); mask(i,j)=nan; end
% exclude central Arctic basin
i=find(Y>=80); mask(i)=nan;
mask(:,1:50)=nan;       % exclude low-latitude Atlantic
mask(:,701:735)=nan;    % exclude low-latitude Pacific

% load model land-sea mask
tmask0=ncread('CREG025_mesh_mask.nc','tmask'); tmask0=squeeze(tmask0(:,:,1));
i=find(tmask0==0); mask(i)=0;

nccreate('regions_mask_8.nc','regions_mask',"Dimensions",{"i",nx,"j",ny});
ncwrite('regions_mask_8.nc','regions_mask',mask);
```

APPENDIX C - ADDITIONAL SCATTER PLOTS

Scatter plots for region means were extremely useful in evaluating the optimal set of grazing and mortality parameters. Christian et al. (2025) show examples of these plots for 'bookend' scenarios that best illustrate the range of outcomes, from low biomass and weak biological drawdown of NO_3 and DIC to high productivity and excessive drawdown. But there were far too many experiments to show them all. These plots are shown here for surface ocean pCO_2, nitrate concentration, and chlorophyll concentration, for the full suite of grazing and mortality parameter experiments. As noted above, some of these experiments have exudation and chlorophyll degradation while others do not (Table 1), but sensitivity to these processes is negligible for the data comparisons shown here (see Appendix A).

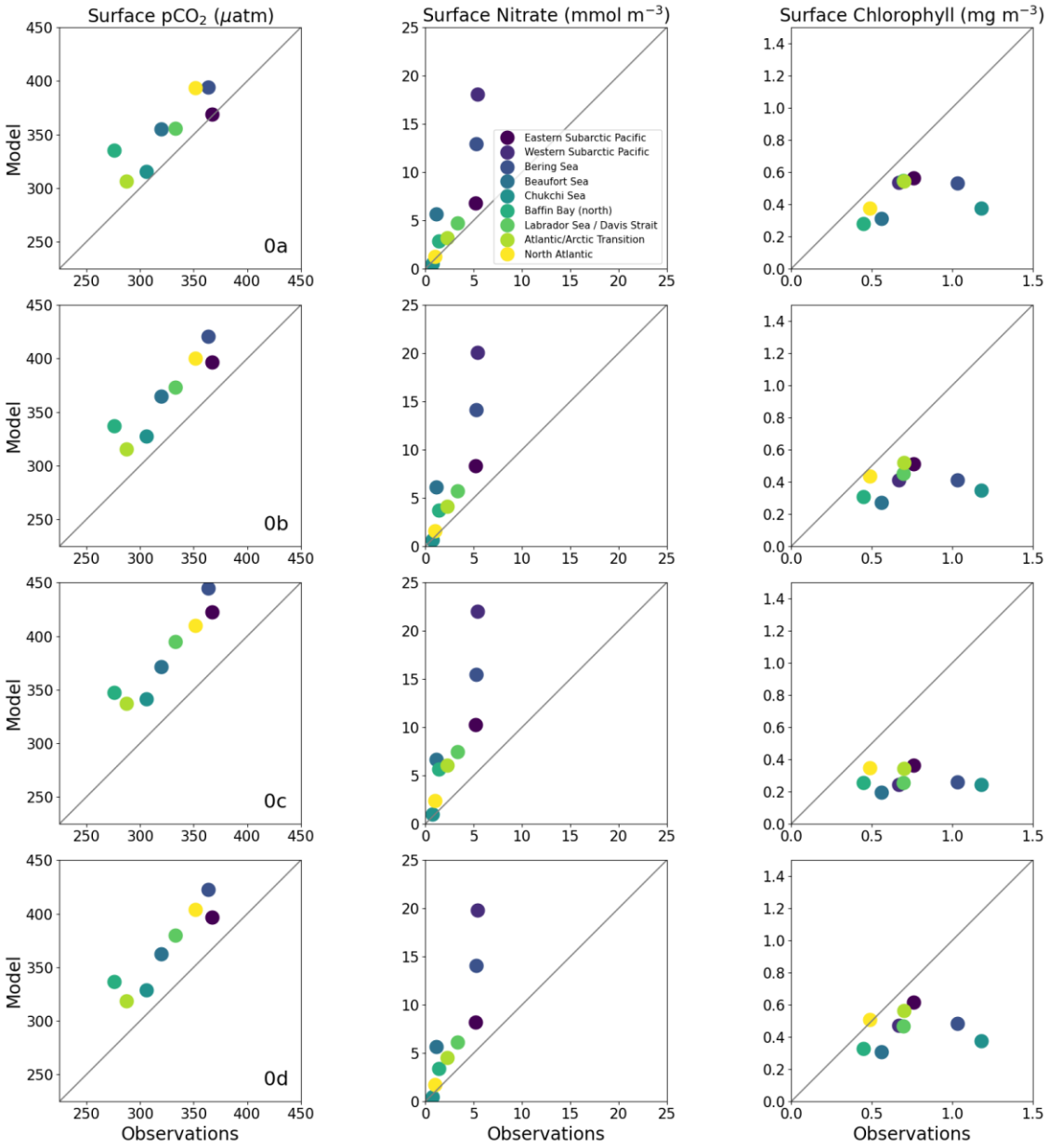
Surface pCO2 (μatm)
Surface Nitrate (mmol m−3)
Surface Chlorophyll (mg m−3)
Model
Observations
0a
0b
0c
0d
Eastern Subarctic Pacific
Western Subarctic Pacific
Bering Sea
Beaufort Sea
Chukchi Sea
Baffin Bay (north)
Labrador Sea / Davis Strait
Atlantic/Arctic Transition
North Atlantic

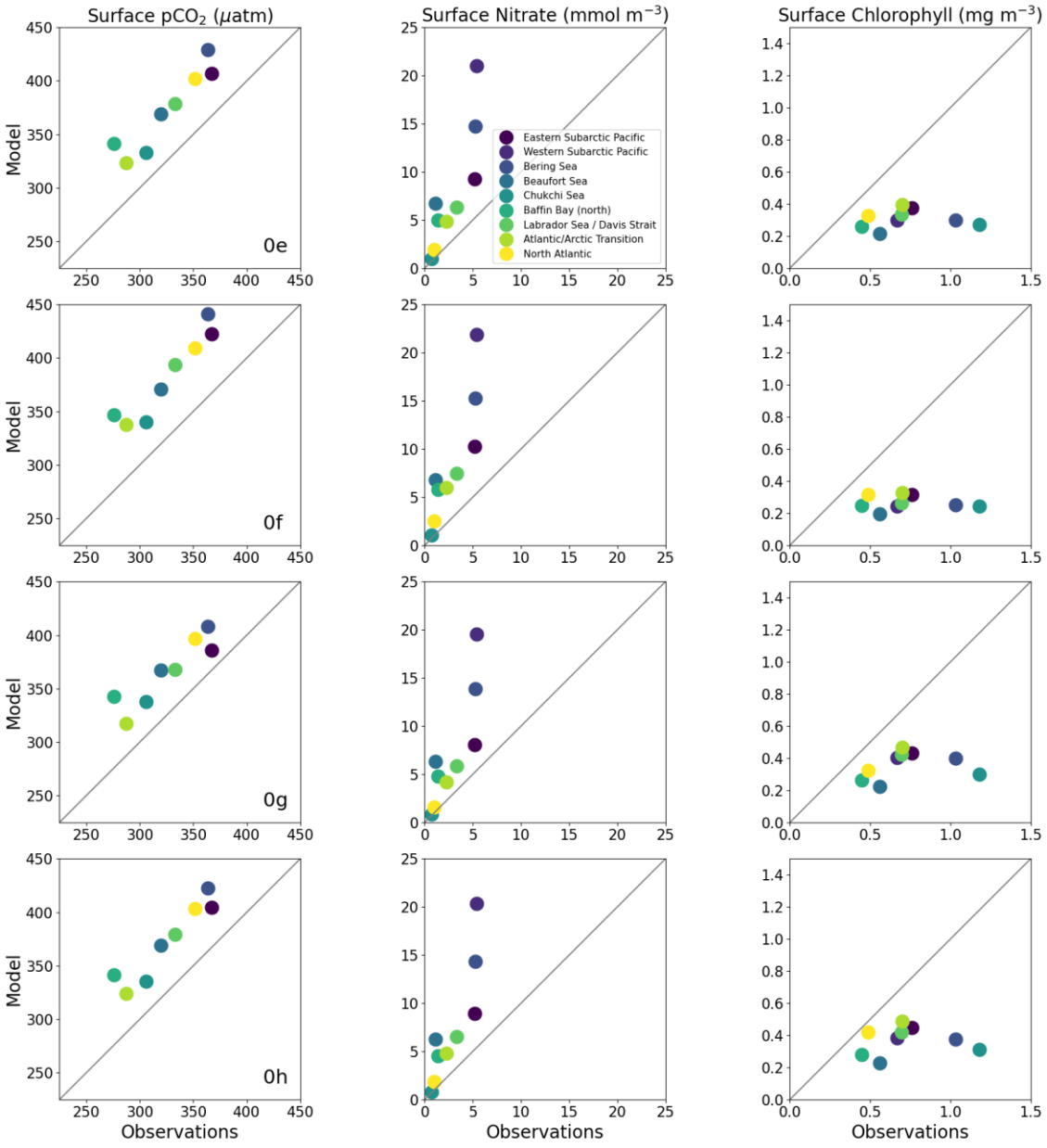
Surface pCO2 (μatm)
Surface Nitrate (mmol m−3)
Surface Chlorophyll (mg m−3)
Model
Observations
0e
0f
0g
0h
Eastern Subarctic Pacific
Western Subarctic Pacific
Bering Sea
Beaufort Sea
Chukchi Sea
Baffin Bay (north)
Labrador Sea / Davis Strait
Atlantic/Arctic Transition
North Atlantic

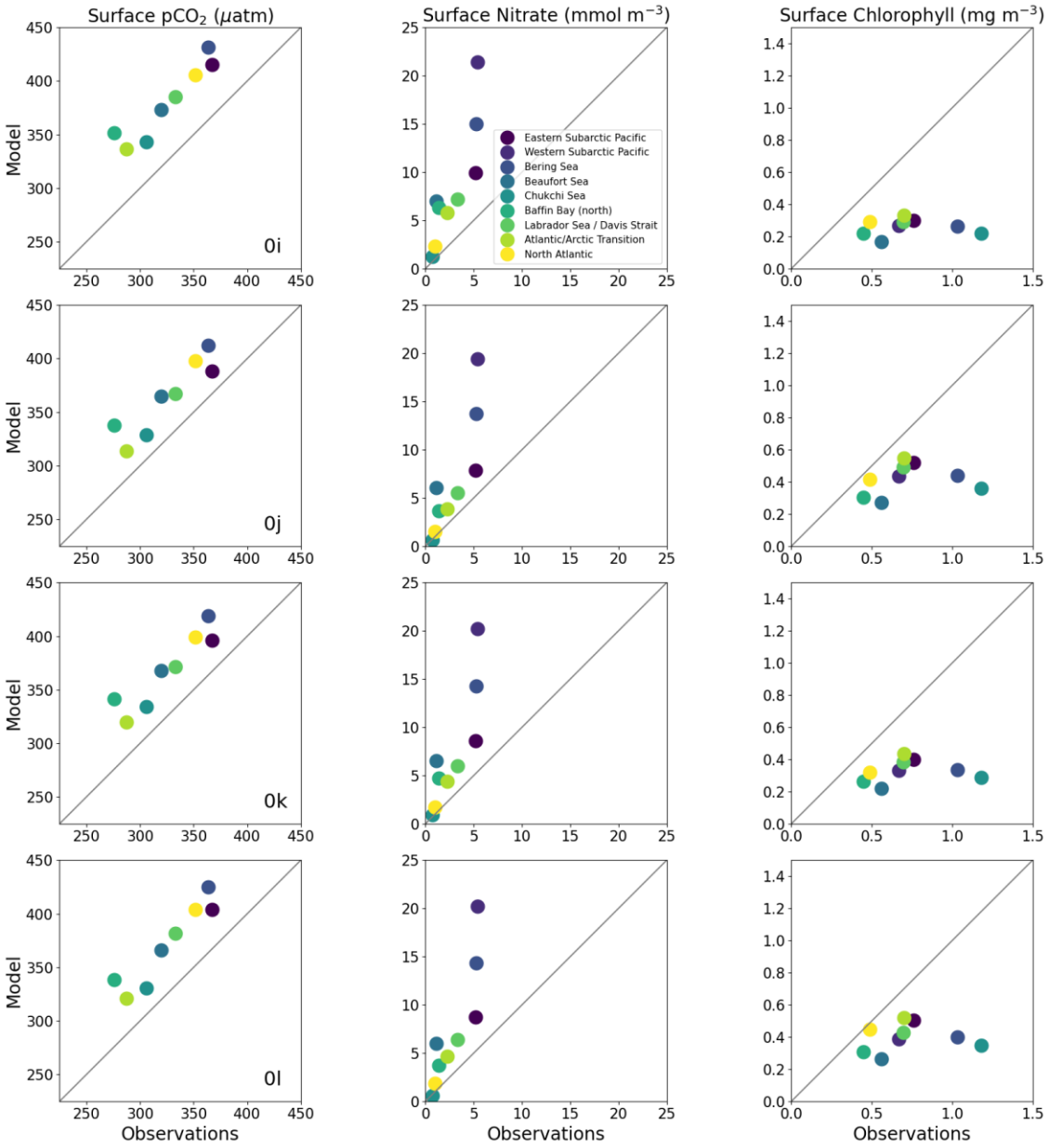
Surface pCO2 (μatm)
Surface Nitrate (mmol m−3)
Surface Chlorophyll (mg m−3)
Model
Observations
0i
0j
0k
0l
Eastern Subarctic Pacific
Western Subarctic Pacific
Bering Sea
Beaufort Sea
Chukchi Sea
Baffin Bay (north)
Labrador Sea / Davis Strait
Atlantic/Arctic Transition
North Atlantic

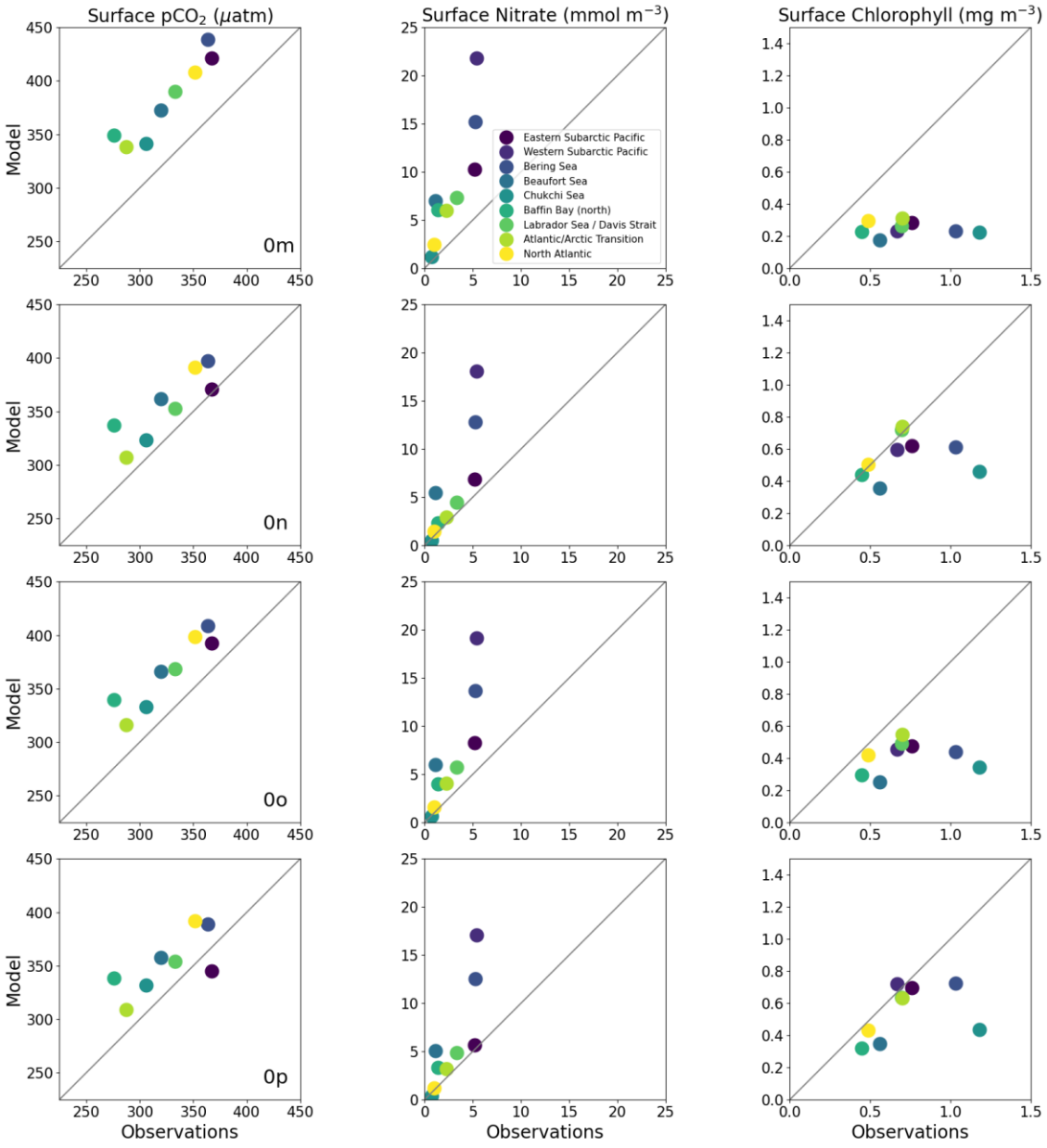
Surface pCO2 (μatm)
Surface Nitrate (mmol m−3)
Surface Chlorophyll (mg m−3)
Model
Observations
0m
0n
0o
0p
Eastern Subarctic Pacific
Western Subarctic Pacific
Bering Sea
Beaufort Sea
Chukchi Sea
Baffin Bay (north)
Labrador Sea / Davis Strait
Atlantic/Arctic Transition
North Atlantic

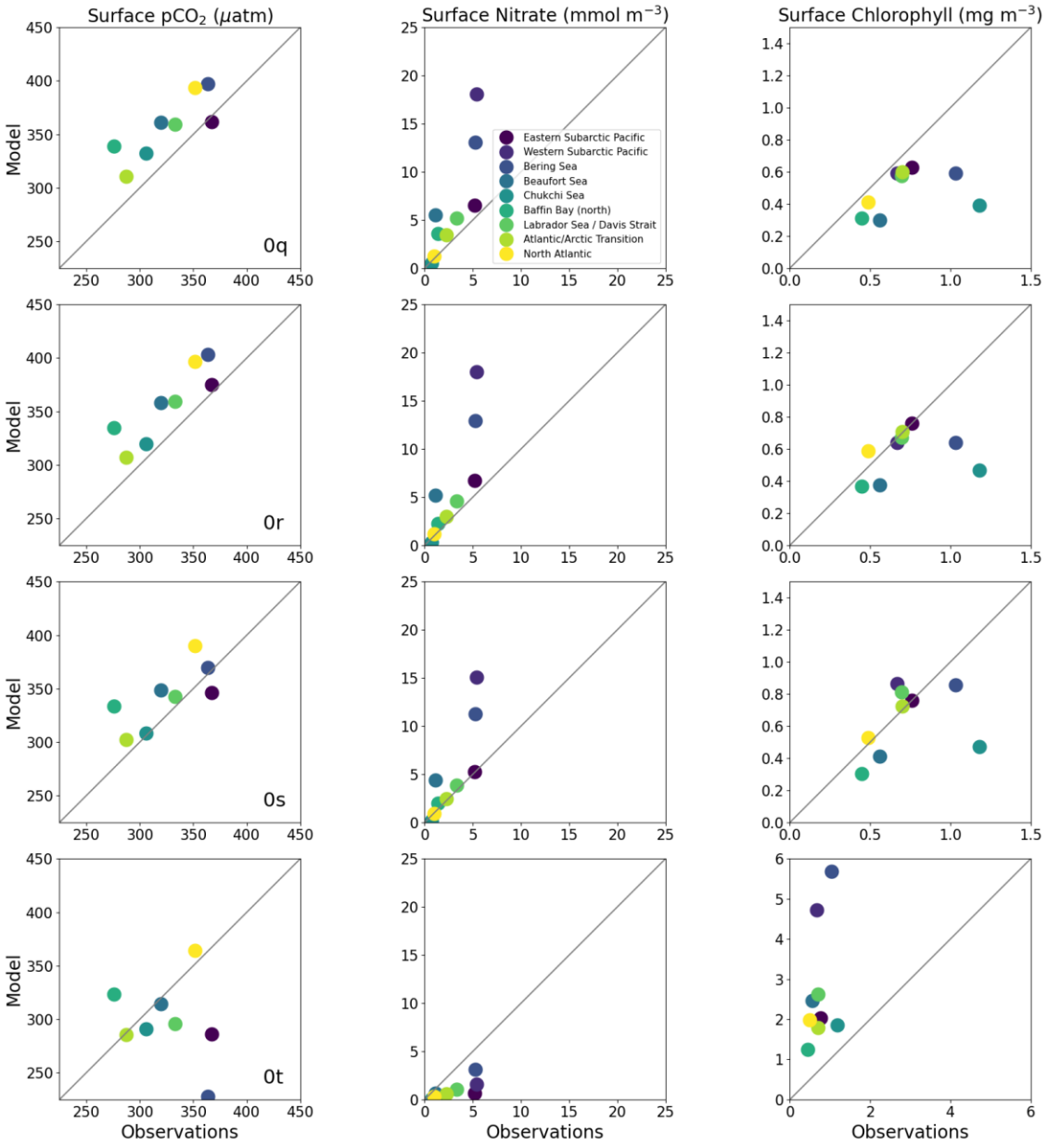
Surface pCO2 (μatm)
Surface Nitrate (mmol m−3)
Surface Chlorophyll (mg m−3)
Model
Observations
0q
0r
0s
0t
Eastern Subarctic Pacific
Western Subarctic Pacific
Bering Sea
Beaufort Sea
Chukchi Sea
Baffin Bay (north)
Labrador Sea / Davis Strait
Atlantic/Arctic Transition
North Atlantic

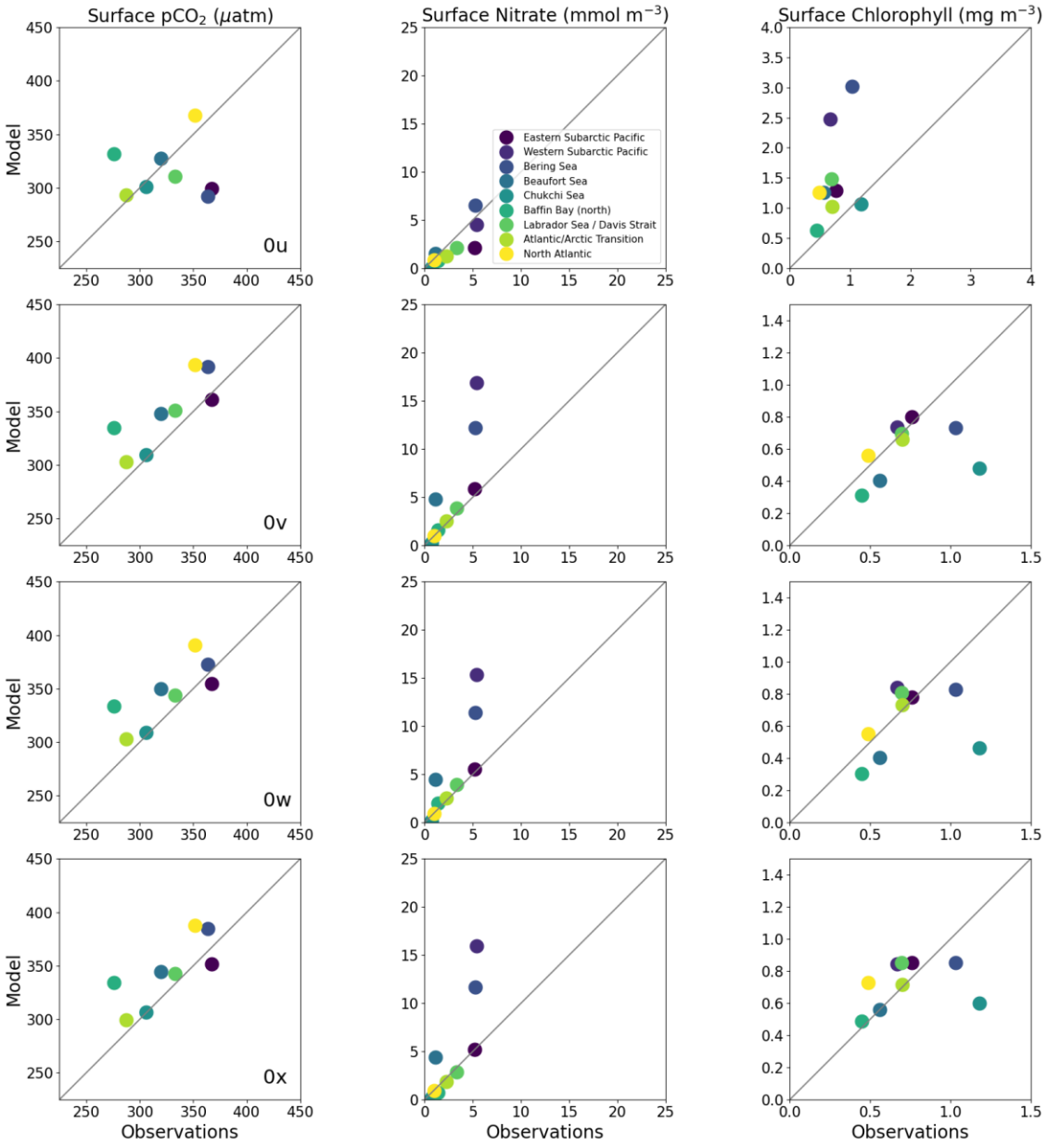
Surface pCO2 (μatm)
Surface Nitrate (mmol m−3)
Surface Chlorophyll (mg m−3)
Model
Observations
0u
0v
0w
0x
Eastern Subarctic Pacific
Western Subarctic Pacific
Bering Sea
Beaufort Sea
Chukchi Sea
Baffin Bay (north)
Labrador Sea / Davis Strait
Atlantic/Arctic Transition
North Atlantic

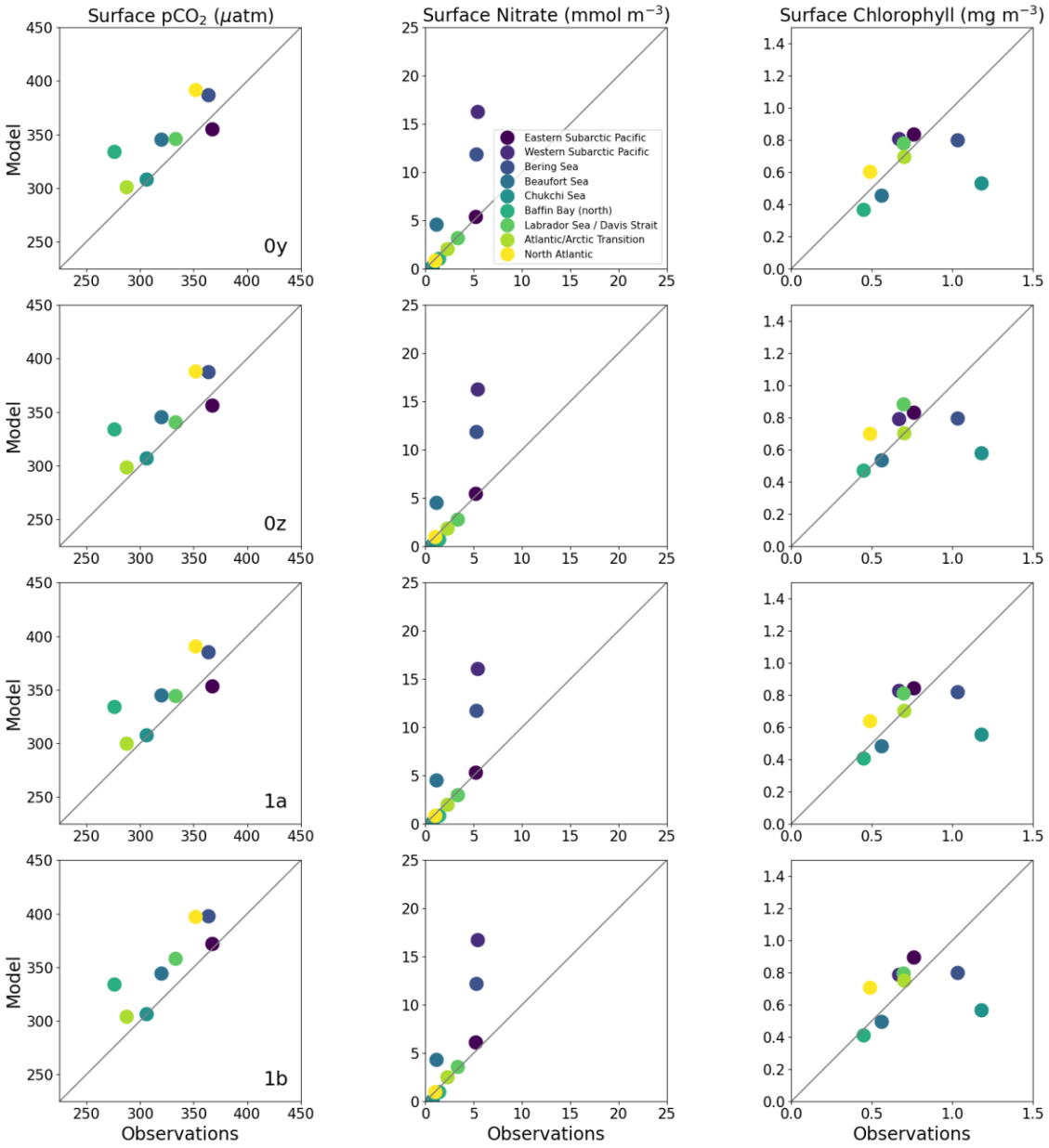
Surface pCO2 (μatm)
Surface Nitrate (mmol m−3)
Surface Chlorophyll (mg m−3)
Model
Observations
0y
0z
1a
1b
Eastern Subarctic Pacific
Western Subarctic Pacific
Bering Sea
Beaufort Sea
Chukchi Sea
Baffin Bay (north)
Labrador Sea / Davis Strait
Atlantic/Arctic Transition
North Atlantic

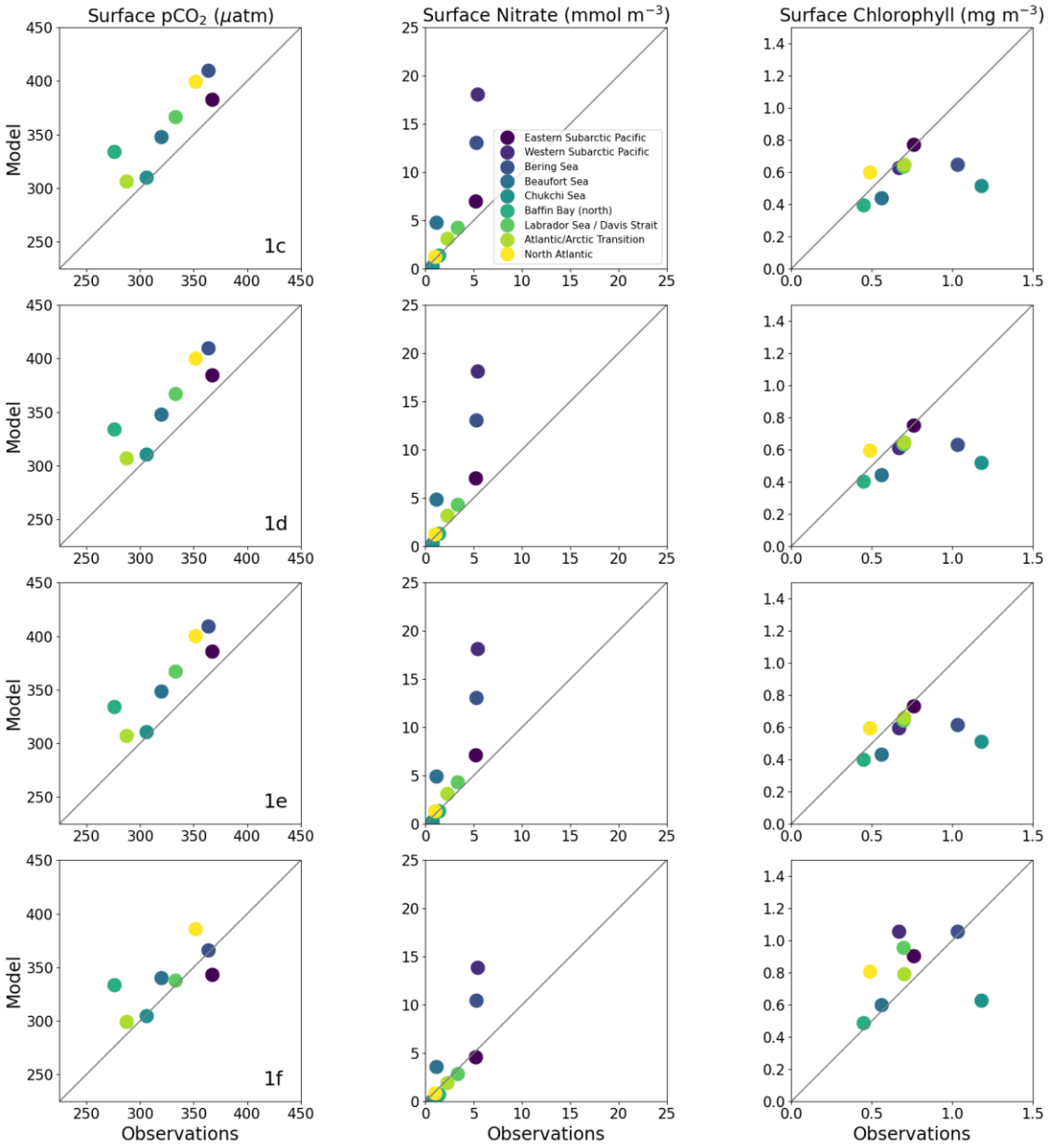
Surface pCO2 (μatm)
Surface Nitrate (mmol m−3)
Surface Chlorophyll (mg m−3)
Model
Observations
1c
1d
1e
1f
Eastern Subarctic Pacific
Western Subarctic Pacific
Bering Sea
Beaufort Sea
Chukchi Sea
Baffin Bay (north)
Labrador Sea / Davis Strait
Atlantic/Arctic Transition
North Atlantic

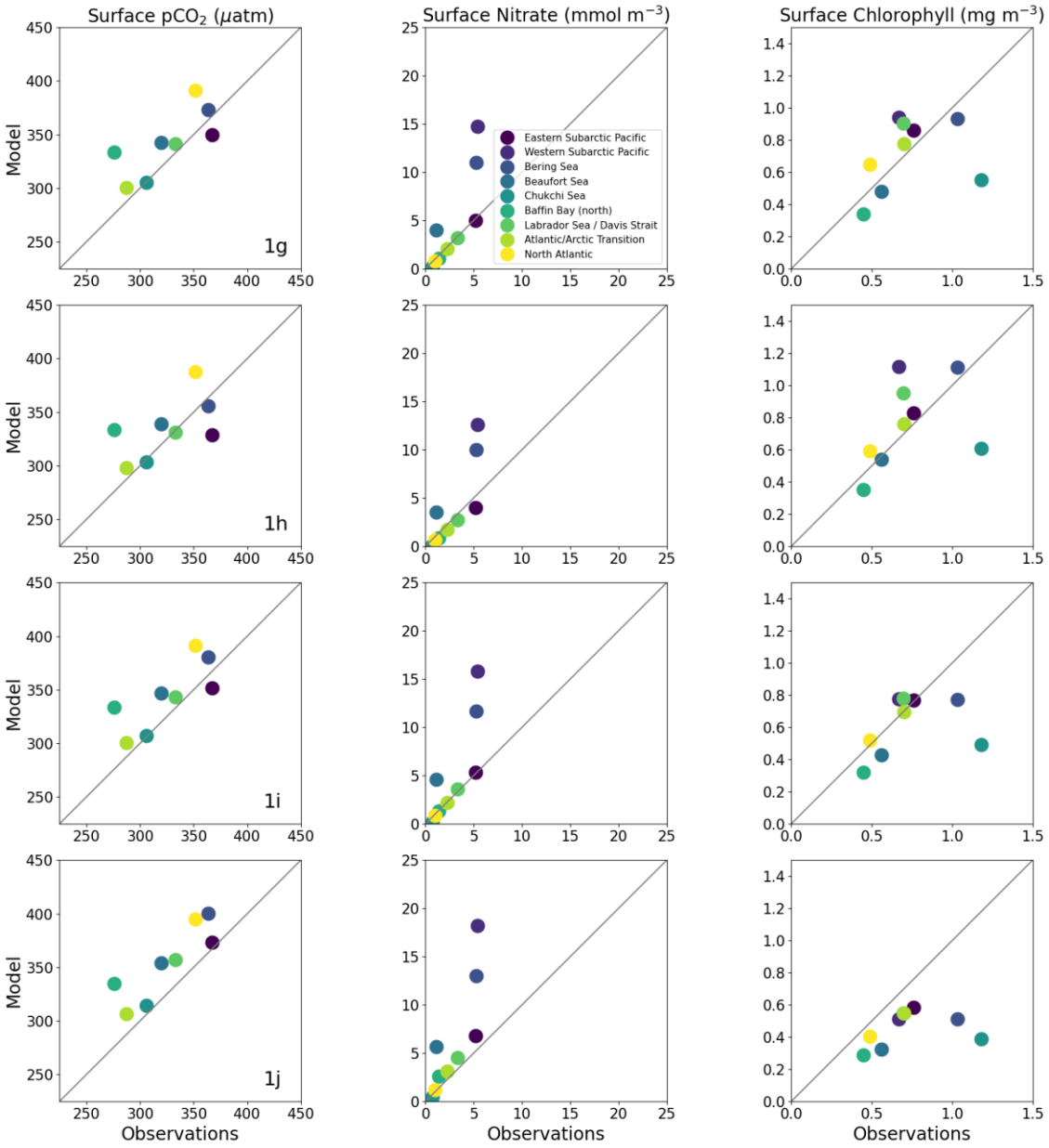
Surface pCO2 (μatm)
Surface Nitrate (mmol m−3)
Surface Chlorophyll (mg m−3)
Model
Observations
1g
1h
1i
1j
Eastern Subarctic Pacific
Western Subarctic Pacific
Bering Sea
Beaufort Sea
Chukchi Sea
Baffin Bay (north)
Labrador Sea / Davis Strait
Atlantic/Arctic Transition
North Atlantic